ISSN 0280–5316
ISRN LUTFD2/TFRT--5693--SE

# Force Estimation and Control in Vehicles and Robots

Alex Alcocer Peñas

Department of Automatic Control
Lund Institute of Technology
October 2002

**Department of Automatic Control**
**Lund Institute of Technology**
**Box 118**
**SE-221 00 Lund Sweden**

*Document name*
MASTER THESIS

*Date of issue*
October 2002

*Document Number*
ISRN LUTFD2/TFRT--5693--SE

*Author(s)*
Alex Alcocer Peñas

*Supervisor*
Rolf Johansson and Anders Robertsson at LTH

*Sponsoring organization*

*Title and subtitle*
Force Estimation and Control in Vehicles and Robots (Kraftestimering och kraftreglering i farkoster och robotar)

*Abstract*
In this master thesis, it will be shown howto estimate the unknown environmental forces acting on diÿerent vehicular and robotic systems. As force sensors are expensive, complex and not suitable to operate in hazardous environments, we present an approach to force estimation using model based observers. Only position measurements are assumed to be available and it will be shown how to use this force estimation to build an improved velocity observer. A force estimator able to follow ramp environmental forces is also introduced. We will pay special attention to stability issues and noise considerations. Simulations will be done using Matlab and Simulink. A parameter identification and force estimation experiment will be done using an industrial robot ABB irb2000.

*Keywords*

*Classification system and/or index terms (if any)*

*Supplementary bibliographical information*

*ISSN and key title*
0280-5316

*ISBN*

*Language*
English

*Number of pages*
67

*Recipient's notes*

*Security classification*

## Acknowledgements

I would like to thank my supervisors in Lund Rolf Johansson and Anders Robertsson for their constant help and support during all my master's thesis. It made me feel very comfortable when I knew where to find an answer for all my questions. I would also like to thank Angel Valera Fernandez, from Universitat Politècnica de València, who during his stay in Lund help me with the robot experiments, Josep M. Fuertes, from Universitat Politècnica de Catalunya, who encouraged me to come to Lund, Leif Andersson for his support with the computers and LaTeX, the "golden ladies" Eva, Agneta and Britt-Marie and all the nice people at the Automatic Control Department of LTH, for making my stay in Lund more pleasant.

*Alex*

# Contents

# 1. Introduction

In many physical systems, such as robots and vehicles, there are unmeasured environmental forces that can modify their expected behavior. As examples of these environmental forces we can consider contact forces for robot manipulators and wind and sea currents for marine vehicles. From the control point of view, these environmental forces are extremely important as they can decrease the control performance and even destabilize the system. The estimation of these environmental forces is the purpose of this Master's thesis.

## 1.1 Problem Formulation

Consider a general dynamic system described by

$$\begin{cases} \dot{x} = f(t, x, u, F) \\ y = h(t, x, u, F) \end{cases} \tag{1.1}$$

where $u$ is the vector of known inputs, $F$ is the vector of unknown inputs (the environmental forces) and $y$ is the measured output of the system. Assuming that velocity measurements are not available, so that the vector $y$ is composed of position measurements only, we want to obtain an estimate $\hat{F}$ of the unknown input $F$.

This is a very general problem but we will concentrate on more specific systems. As example of linear systems we will study the rigid body and a damped rigid body. As examples of nonlinear systems, we will consider a simplified model of a ship and a robot manipulator.

## 1.2 Force Sensing and Control

Force control is quite a new field and it is becoming more important everyday. In the robotics case, there are many industrial applications in which we may need to control the forces between the robot and its environment. Consider for instance assembly operations or tasks that involve the interaction of the robot with fragile objects. For an understanding of force sensors and force control techniques see [13], [14], [12].The main objective of this thesis is to develop a method to estimate these environmental forces, so that they afterwards can be used for control purposes.

One of the first questions that we might think of is *why don't we use a force sensor?* Force sensors have drawbacks that make them not suitable in some applications. For example:

- High prize;
- Not applicable where we would like the force measurement;
- High noise-to-signal ratio;
- Complexity;

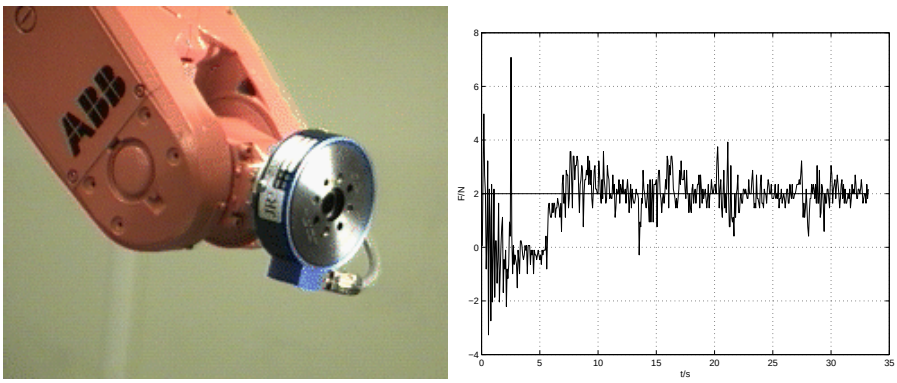


**Figure 1.1** Force sensor used in the robot manipulator and noisy force signal

- Sensitive to temperature and environment changes;
- Not able to work in hazardous environments;

There are other situations in which force sensing may be not possible. For example, in the case of ships, there exist no sensors to measure the sea currents and its interaction with the ship dynamics, even though they can have extremely importance in the control performance. In Figure 1.1, we can see a picture of a force sensor attached to a robot manipulator and its sensed signal.

## 1.3 Velocity Measurements and *"Dirty Derivatives"*

Another question that needs to be answered is *why don't we use velocity measurements?* We have assumed that there are not velocity sensors available but, is this a real situation? In most industrial robotic manipulators there are not velocity sensors, but only position measurements. However, velocity estimates are needed for control tasks. In these cases, a common technique to obtain velocity estimates is simply to differentiate position measurements. This is also known as *dirty derivatives* and has some drawbacks that must be considered. Very insignificant noises in position measurements can lead to completely distorted and *dirty* velocity estimates. As a clear example of this problem we will see later in this thesis how a slight nonlinearity in the resolvers of the robot system produced an important distortion that needed to be compensated (see Fig. 1.2). Moreover, there are other situations in which velocity sensing is not trivial. In the ship case consistent velocity measurements are very hard to obtain due to the strong effect of sea currents. A different approach to obtain velocity estimates is the use of observers.

## 1.4 Observers

In many applications where sensors are not available it is necessary to estimate some unmeasured quantities of the system. An observer is an

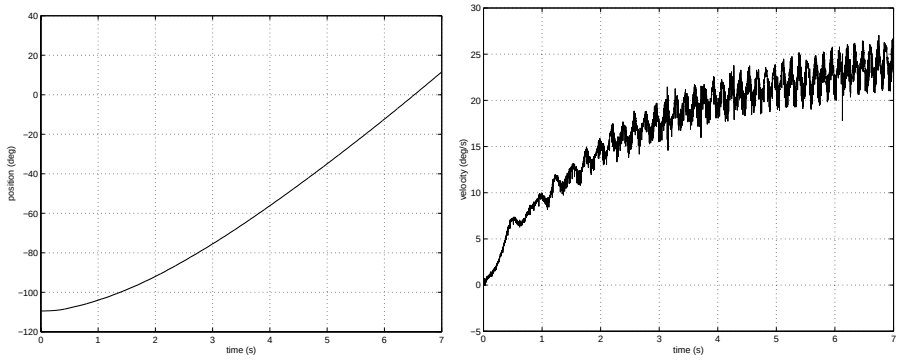


**Figure 1.2** Position measurement and dirty velocity estimates by differentiation

algorithm that reconstruct the unmeasured internal states of a system from the measured output. In the linear case the observer theory is well investigated and the observability and detectability properties are closely connected to the existence of observers with strong convergence properties. However, in the nonlinear case, the existence of a solution is not assured. The design of nonlinear observers is not straight forward and requires the use of a wide number of techniques as for instance *Lyapunov stability theory* or *Passivity formalism*.

### Observers for Linear Systems

Consider the linear system

$$\begin{cases} \dot{x} = Ax + Bu \\ y = Cx \end{cases} \tag{1.2}$$

Under observability/detectability assumptions on the pair $[A, C]$, an observer for the system in (1.2) can be constructed as

$$\begin{cases} \dot{\hat{x}} = A\hat{x} + Bu + K(y - \hat{y}) \\ \hat{y} = C\hat{x} \end{cases} \tag{1.3}$$

where $K(y-\hat{y})$ is the linear output injection. If the gain matrix $K$ is chosen such that $(A-KC)$ is *Hurwitz*, then the error dynamics are asymptotically stable, that is $lim_{t\to\infty}\ \hat{x}(t) = x(t)$.

### Observers for Nonlinear Systems

This is a field in which there is still much to investigate. The design of nonlinear observers does not have a systematic solution, and we might have to try different techniques before being successful. One approach to the problem makes use of the linearization of the system around a different number of design points and uses a different linear observer in each region. With this method we can use the well known techniques for linear systems but on the other hand we will not be able to assure asymptotic stability anymore, but only local stability around each of the design points. As we will see when studying the ship dynamics, another drawback that arises with the linearization approach is that as the number of linearization points increases so does the quantitative complexity of the observer.

We might look forward to obtain a more compact and usable observer by increasing its qualitative complexity. Given a nonlinear system

$$\begin{cases} \dot{x} = f(x,u) \\ y = h(x,u) \end{cases} \tag{1.4}$$

where the structure of $f$ and $h$ is assumed to be known. It is possible to think of an observer copying the dynamics of (1.4) as

$$\begin{cases} \dot{\hat{x}} = f(\hat{x},u) + K(y-\hat{y}) \\ \hat{y} = h(\hat{x},u) \end{cases} \tag{1.5}$$

In this case, in order to assure the stability of the observer error dynamics we need to make use of *Lyapunov stability analysis* or *Passivity*. Despite the fact it seems a quite simple problem there might be no solution to an asymptotically stable observer. For a detailed study on nonlinear observers and control see for example [4].

## 1.5 Lyapunov Stability Theory

This is one of the basic tools when dealing with nonlinear systems and it will be widely used in the course of this thesis. In this section we will just point out the basic theorem of *Lyapunov Stability Theory*. For a deeper understanding and proofs see for example [22] or [23].

THEOREM 1.1
Let $x = 0$ be an equilibrium point for $\dot{x} = f(x)$ and let $V : D \to \mathbf{R}$ be a continuously differentiable scalar function on a neighborhood $D$ of $x = 0$ such that

$$V(0) = 0 \quad \text{and} \quad V(x) > 0 \quad \text{in} \quad D - \{0\} \tag{1.6}$$

$$\dot{V}(x) \leq 0 \quad \text{in} \quad D \tag{1.7}$$

then, $x = 0$ is stable. Moreover, if

$$\dot{V}(x) < 0 \quad \text{in} \quad D - \{0\} \tag{1.8}$$

then $x = 0$ is asymptotically stable in $D$. □

## 1.6 Passivity Theory

Passivity theory is a very powerful branch of system theory that can give many intuitive insights over the behavior and stability of physical systems. We will mention some basic definitions that are going to be used in the sequel. For a good overview over passivity and how it can be used for control purposes see for example [24].

DEFINITION 1.1—DISSIPATIVITY
Consider a dynamical system $\Sigma$ with equal input and output dimensions

$$\Sigma : \begin{cases} \dot{x} = f(x,u), & x \in \mathrm{R}^n, \quad u \in \mathrm{R}^p \\ y = h(x,u), & y \in \mathrm{R}^p \end{cases} \tag{1.9}$$

If there exist a function $w(u,y)$, the *supply rate*, and a positive definite function $S(x) \geq 0$, the *storage function*, such that

$$S(x(t)) - S(x(0)) \leq \int_0^t w(u(\tau), y(\tau)) d\tau \tag{1.10}$$

for all admissible inputs $u$ and all $t \geq 0$, then the system is called *dissipative*. □

DEFINITION 1.1—PASSIVITY
A system $\Sigma$ is said to be *passive* if it is dissipative with the supply rate $w(u,y) = u^T y$. The system (1.9) is passive if

$$u^T y \geq 0 \tag{1.11}$$

□

# 2. Force Observer for Linear Systems

## 2.1 Introduction

In this chapter we are going to introduce a force observer for linear systems. We will first study a general second order dynamic system and find a solution to the force estimation problem. Then we will apply it to common linear systems as a rigid-body and a damped rigid-body. Comments about the behavior of the force estimation error will be given for each case.

Force estimation using $H^\infty$ sensitivity techniques has been studied by Ohishi and his coworkers in [3]. Observer based force estimation has been introduced by Hacksel and Salcudean in [1]. In this thesis we will continue this approach giving new results and extending it to the nonlinear dynamics case.

## 2.2 System Model and Problem Formulation

Consider a second order linear system with an environmental force $F$ as an unknown input. We can write a state space representation as

$$\begin{cases} \dot{x} = Ax + B(u + F) \\ y = Cx \end{cases} \tag{2.1}$$

where,

$$x = \begin{pmatrix} x_1 \\ x_2 \end{pmatrix}, \quad A = \begin{pmatrix} a_{11} & a_{12} \\ a_{21} & a_{22} \end{pmatrix}, \quad B = \begin{pmatrix} 0 \\ b \end{pmatrix}, \quad C = \begin{pmatrix} 1 & 0 \end{pmatrix}$$

We assume that only $x_1$ is available to measure. The environmental force $F$ acts in the same way as $u$, that is only on $x_2$. We want to obtain an estimate $\hat{F}$ of the environmental force.

## 2.3 General Solution

The main idea is to build an observer for the linear system in which the environmental force is not considered. The mismatch between the observer and the real system will produce structured estimation errors that will make possible to deduce the environmental force.

A linear observer for the system in (2.1) in which the environmental force has not been considered can be written as

$$\begin{cases} \dot{\hat{x}} = A\hat{x} + Bu + K(y - \hat{y}) \\ \hat{y} = C\hat{x} = \hat{x}_1 \end{cases} \tag{2.2}$$

with

$$\hat{x} = \begin{pmatrix} \hat{x}_1 \\ \hat{x}_2 \end{pmatrix}, \quad K = \begin{pmatrix} K_1 \\ K_2 \end{pmatrix}$$

Lets define $\tilde{x} = x - \hat{x} = [\tilde{x}_1 \;\; \tilde{x}_2]^T$. Then from (2.1) and (2.2) we can obtain the error dynamics

$$\dot{\tilde{x}} = (A - KC)\tilde{x} + BF \tag{2.3}$$

lets define

$$\mathcal{A} = A - KC = \begin{pmatrix} a_{11} - K_1 & a_{12} \\ a_{21} - K_2 & a_{22} \end{pmatrix}$$

Then we can split (2.3) and write

$$\dot{\tilde{x}}_1 = a_{11}\tilde{x}_1 + a_{12}\tilde{x}_2 - K_1\tilde{x}_1 \tag{2.4}$$
$$\dot{\tilde{x}}_2 = a_{21}\tilde{x}_1 + a_{22}\tilde{x}_2 + bF - K_2\tilde{x}_1 \tag{2.5}$$

from (2.4) is obvious that

$$\tilde{x}_2 = \frac{1}{a_{12}}(\dot{\tilde{x}}_1 - a_{11}\tilde{x}_1 + K_1\tilde{x}_1) \tag{2.6}$$

Deriving (2.4) and using (2.5)-(2.6) we can obtain the equation for the dynamics of $\tilde{x}_1$

$$\boxed{\Lambda_2 \, \dddot{\tilde{x}}_1 + \Lambda_1 \, \ddot{\tilde{x}}_1 + \Lambda_0 \, \dot{\tilde{x}}_1 = F} \tag{2.7}$$

with

$$\begin{cases} \Lambda_2 = \dfrac{1}{a_{12}b} \\ \Lambda_1 = \dfrac{K_1 - \mathrm{tr}A}{a_{12}b} \\ \Lambda_0 = \dfrac{K_2 a_{12} - K_1 a_{22} + \det A}{a_{12}b} \end{cases} \tag{2.8}$$

If

$$\Lambda_2, \;\; \Lambda_1, \;\; \Lambda_0 \geq 0 \tag{2.9}$$

the matrix $\mathcal{A}$ is *Hurwitz* and $\tilde{x}_1$ shows an interesting property. We can see in (2.7) that the estimation error $\tilde{x}_1$ behaves as a damped spring mass system driven by the environmental force $F$. This is one of the main results from which the force estimator will be derived. There exist an equilibrium point of (2.7) at $\tilde{x}_1 = \Lambda_0^{-1}F$. Hence, when $F$ is enough slow time varying, under assumption (2.9), we claim that is possible to obtain an estimate of the environmental force $\hat{F}$ as

$$\boxed{\hat{F} = \Lambda_0 \, \tilde{x}_1} \tag{2.10}$$

Now consider the system formed by (2.3) and (2.10) with input $F$ and output $\hat{F}$

$$\begin{cases} \dot{\tilde{x}} = (A - KC)\tilde{x} + BF \\ \hat{F} = \Lambda_0 C\tilde{x} \end{cases} \tag{2.11}$$

we can obtain its transfer function

$$\mathcal{G}_{\hat{F}}(s) = \Lambda_0 C(sI - A + KC)^{-1}B \tag{2.12}$$

and for constant environmental forces we want $\hat{F} \equiv F$, so that the static gain of $\mathcal{G}_{\hat{F}}(s)$ should be the identity

$$\begin{aligned} \mathcal{G}_{\hat{F}}(0) &= I \quad \Rightarrow \quad \Lambda_0 C(-A + KC)^{-1}B = I \quad \Rightarrow \\ \Lambda_0 &= \left[C(-A + KC)^{-1}B\right]^{-1} \end{aligned} \tag{2.13}$$

which in our case becomes

$$\begin{aligned} \Lambda_0 &= \left[ \begin{pmatrix} 1 & 0 \end{pmatrix} \begin{pmatrix} K_1 - a_{11} & -a_{12} \\ K_2 - a_{21} & -a_{22} \end{pmatrix}^{-1} \begin{pmatrix} 0 \\ b \end{pmatrix} \right]^{-1} \\ &= \left[ \begin{pmatrix} 1 & 0 \end{pmatrix} \frac{1}{K_2 a_{12} - K_1 a_{22} + \det A} \begin{pmatrix} -a_{22} & a_{12} \\ a_{21} - K_2 & K_1 - a_{11} \end{pmatrix} \begin{pmatrix} 0 \\ b \end{pmatrix} \right]^{-1} \\ &= \frac{K_2 a_{12} - K_1 a_{22} + \det A}{a_{12} b} \end{aligned} \tag{2.14}$$

Hence, using (2.13) we have arrived to the same result as in (2.8).

**Summary**

Given a linear system with the structure of (2.1) it is possible to obtain an estimate of the environmental force by using

$$\begin{cases} \dot{\hat{x}} = A\hat{x} + Bu + K\tilde{x}_1 \\ \tilde{x}_1 = x_1 - \hat{x}_1 \\ \hat{F} = \Lambda_0 \ \tilde{x}_1 \end{cases} \tag{2.15}$$

with $\hat{x} = [\hat{x}_1 \ \hat{x}_2]^T$, $\Lambda_0$ as in (2.8) and $K = [K_1 \ K_2]^T$ such that (2.9) is fulfilled.

**Stability Considerations**

It is important to notice that in this first observer (2.2) we don't want to estimate the states of the system. Using the terms observer and observer error dynamics can be confusing and we have to be careful. We call it observer because it has its structure, but it is not used as a state estimator but as sensor for disturbance forces. Hence, we don't expect the estimation error to converge to zero. We expect that this observer has a bounded error necessary to perform the force estimation. First we will show how for bounded environmental forces the estimation error remains bounded and we will find an expression for this boundary. Later, a final statement on passivity will be introduced.

Consider the following Lyapunov function candidate

$$V = \tilde{x}^T P \tilde{x} \tag{2.16}$$

with $P = P^T > 0$. The time derivative of $V$ along the solution of (2.3) is

$$\begin{aligned} \dot{V} &= \dot{\tilde{x}}^T P\tilde{x} + \tilde{x}^T P\dot{\tilde{x}} \\ &= \tilde{x}^T(\mathcal{A}^T P + P\mathcal{A})\tilde{x} + 2\tilde{x}^T PBF \end{aligned} \tag{2.17}$$

the matrix $\mathcal{A}$ is *Hurwitz* under assumption (2.9). Hence, there exists symmetric positive definite matrices $Q$ and $P$ such that $\mathcal{A}^T P + P\mathcal{A} = -Q$. Then we can write

$$\dot{V} = \underbrace{-\tilde{x}^T Q\tilde{x}}_{1} + \underbrace{2\tilde{x}^T PBF}_{2} \tag{2.18}$$

The first term of (2.18) is negative definite and will tend to bring the estimation error $\tilde{x}$ to zero. The second term is not definite so it can be positive and tend to increase $\tilde{x}$. The first term contains a quadratic term in $\tilde{x}$ so its stabilizing effect will be more important as $\tilde{x}$ grows. We see that there is a balance between both terms of the equation, so that the first term will always keep $V$ from growing more than a certain finite boundary determined by $F$. Lets now find an expression for this boundary.

$$\begin{aligned} \dot{V} &\leq -\lambda_{min}(Q)\|\tilde{x}\|^2 + 2\|\tilde{x}\|\|PB\|\|F\| \\ &= -\Delta_a^2 + \Delta_a\Delta_b \end{aligned} \tag{2.19}$$

where $\Delta_a = \sqrt{\lambda_{min}(Q)}\|\tilde{x}\|$, $\Delta_b = \frac{2\|PB\|\|F\|}{\sqrt{\lambda_{min}(Q)}}$, and $\lambda_{min}$ represents the minimum eigenvalue. Using completion of squares we can write

$$\dot{V} \leq -\Delta_a^2 + \Delta_a\Delta_b \leq -\frac{1}{2}\Delta_a^2 + \Delta_c\Delta_b^2 \tag{2.20}$$

this inequality holds if $\Delta_c = \frac{1}{2}$. Moreover,

$$V \geq \lambda_{min}(P)\|\tilde{x}\|^2 \quad \longrightarrow \quad \|\tilde{x}\|^2 \leq \frac{1}{\lambda_{min}(P)}V \tag{2.21}$$

then

$$\begin{aligned} \dot{V} &\leq -\frac{1}{2}\Delta_a^2 + \frac{1}{2}\Delta_b^2 \\ &= -\frac{1}{2}\lambda_{min}(Q)\|\tilde{x}\|^2 + \frac{2\|PB\|^2}{\lambda_{min}(Q)}\|F\|^2 \\ &\leq -\frac{1}{2}\frac{\lambda_{min}(Q)}{\lambda_{min}(P)}V + \frac{2\|PB\|^2}{\lambda_{min}(Q)}\|F\|^2 \\ &= -\varepsilon V + \gamma\|F\|^2 \end{aligned} \tag{2.22}$$

where

$$\varepsilon = \frac{1}{2}\frac{\lambda_{min}(Q)}{\lambda_{min}(P)} \qquad \gamma = \frac{2\|PB\|^2}{\lambda_{min}(Q)}$$

The solution to the differential equation of (2.22) can be written and systematically bounded by

$$\begin{aligned} V(t) &\leq e^{-\varepsilon t}V(0) + \int_0^t \gamma\ e^{-\varepsilon(t-s)}\|F(s)\|^2 \mathrm{d}s \\ &\leq e^{-\varepsilon t}V(0) + \gamma\|F\|_\infty^2 \int_0^t e^{-\varepsilon(t-s)}\mathrm{d}s \\ &= e^{-\varepsilon t}V(0) + \frac{\gamma}{\varepsilon}(1-e^{-\varepsilon t})\|F\|_\infty^2 \\ &\leq e^{-\varepsilon t}V(0) + \frac{\gamma}{\varepsilon}\|F\|_\infty^2 \end{aligned} \tag{2.23}$$

where $\|F\|_\infty = \sup_{t\geq 0}\|F(t)\|$.

Hence, given a bounded environmental force, we have obtained a boundary for the estimation error $\tilde{x}$.

## 2.4 Force Estimation Error Dynamics

It has been shown how the position estimation error of the first observer behaves as a damped spring mass system driven by the environmental force. Applying *Laplace* transformation we can rewrite (2.7) in a transfer function form

$$\tilde{X}_1(s) = \frac{1}{\Lambda_2 s^2 + \Lambda_1 s + \Lambda_0} F(s) \tag{2.24}$$

From (2.7) and (2.10) we can obtain an expression of the force estimation error

$$\begin{aligned} \tilde{F} = F - \hat{F} \ &= \Lambda_2\ddot{\tilde{x}}_1 + \Lambda_1\dot{\tilde{x}}_1 + \Lambda_0\tilde{x}_1 - \Lambda_0\tilde{x}_1 \\ &= \Lambda_2\ddot{\tilde{x}}_1 + \Lambda_1\dot{\tilde{x}}_1 \end{aligned} \tag{2.25}$$

which can be written in transfer function form

$$\tilde{F}(s) = s(\Lambda_2 s + \Lambda_1)\tilde{X}_1(s) \tag{2.26}$$

From (2.24) and (2.26) we can find the transfer function between $\tilde{F}$ and $F$

$$\mathcal{H}(s) = \frac{\tilde{F}(s)}{F(s)} = \frac{s(\Lambda_2 s + \Lambda_1)}{\Lambda_2 s^2 + \Lambda_1 s + \Lambda_0} \tag{2.27}$$

We can also obtain the transfer function $\mathcal{H}(s)$ by considering the system

$$\begin{cases} \dot{\tilde{x}} = (A - KC)\tilde{x} + BF \\ \tilde{F} = F - \Lambda_0 C\tilde{x} \end{cases} \tag{2.28}$$

with input $F$ and output $\tilde{F}$. Then,

$$\mathcal{H}(s) = \left[I - \Lambda_0 C(sI - A + KC)^{-1}B\right] \tag{2.29}$$

which will yield to the same result as in (2.27).

$\mathcal{H}(s)$ is a strictly stable transfer function for all $\Lambda_2, \Lambda_1, \Lambda_0 > 0$. It has one zero at $s = 0$ which shows that the force estimation error converges to zero for constant environmental forces. Moreover, we see how the parameters $\Lambda_i$ contain all the information about the behavior of $\tilde{F}$; and, according to (2.8), by choosing appropriate observer gains $K_1$ and $K_2$ we have the possibility to shape these dynamics. This a good result but we can still want $\mathcal{H}(s)$ to fulfill other properties regarding passivity or positive realness of the estimator.

DEFINITION 2.1
[23, page 127] A transfer function $g(s)$ is *positive real* if

$$Re[g(s)] \geq 0 \quad \text{for all} \quad Re[s] \geq 0 \tag{2.30}$$

It is *strictly positive real* if $g(p - \varepsilon)$ is positive real for some $\varepsilon > 0$. □

Direct application of Definition 2.1 to check positive realness is often difficult for high order transfer functions. The following theorem can be used instead.

THEOREM 2.1
[23, page 128] A transfer function $g(s)$ is strictly positive real (SPR) if and only if

i) $g(s)$ is a strictly stable transfer function

ii) the real part of $g(s)$ is strictly positive along the $jw$ axis,i.e.,

$$\forall w \geq 0 \quad Re[g(jw)] > 0 \tag{2.31}$$

□

Consider the force estimation error transfer function $\mathcal{H}(s)$, we have

$$\begin{aligned} \mathcal{H}(jw) &= \frac{-w^2\Lambda_2 + jw\Lambda_1}{-w^2\Lambda_2 + jw\Lambda_1 + \Lambda_0} \\ &= \frac{w^2(\Lambda_1^2 - \Lambda_2\Lambda_0 + w^2\Lambda_2^2) + j(w\Lambda_1\Lambda_2)}{(\Lambda_0 - w^2\Lambda_2)^2 + (w\Lambda_1)^2} \end{aligned} \tag{2.32}$$

and

$$\text{Re}[\mathcal{H}(jw)] = \frac{w^2(\Lambda_1^2 - \Lambda_2\Lambda_0 + w^2\Lambda_2^2)}{(\Lambda_0 - w^2\Lambda_2)^2 + (w\Lambda_1)^2} \tag{2.33}$$

From (2.33) we see that if

$$\Lambda_1^2 > \Lambda_2\Lambda_0 \quad \text{or} \tag{2.34}$$

$$(K_1 - \text{tr}A)^2 > K_2 a_{12} - K_1 a_{22} + \det A \tag{2.35}$$

then $\text{Re}[\mathcal{H}(jw)] > 0$. Hence, for $K_1$ and $K_2$ fulfilling (2.35), and according to Theorem 2.1, $\mathcal{H}(s)$ is a strictly positive real (SPR) transfer function. It can be shown that for linear systems this is the same to say that there is a *Passive* mapping between $F$ and $\tilde{F}$. In Figure 2.1, we can see a Bode and Nyquist plot of $\mathcal{H}(s)$ in which the SPR properties can be checked graphically.

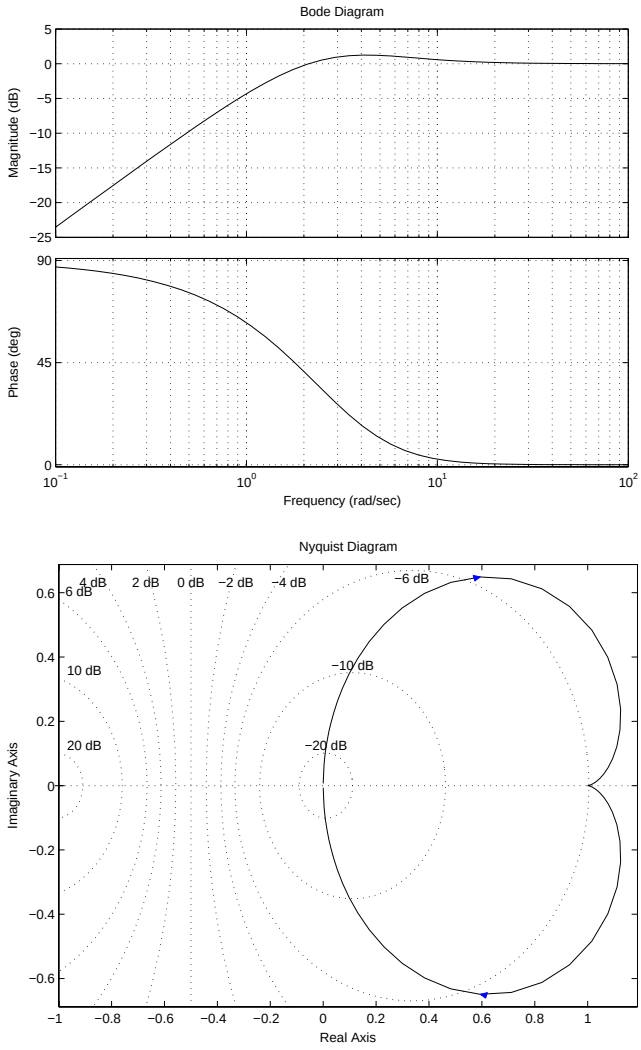


**Figure 2.1** Bode and Nyquist plots of $\mathcal{H}(s)$ whit $\Lambda_2 = 1$, $\Lambda_1 = 6$ and $\Lambda_0 = 9$. Parameters obtained when studying a rigid body with mass $m = 1$ and observer gain $K = [6 \quad 9]^T$. We can see the high pass characteristic of $\mathcal{H}(s)$. $K$ is such that fulfills (2.35).Hence, SPR can be checked noticing that the Nyquist plot never enters the left half plane.

## 2.5 Example I: Rigid Body

Consider a rigid body with mass $m$, position $q$, input force $u$ and unknown environmental force $F$ (see Fig. 2.2)

$$m\ddot{q} = u + F \tag{2.36}$$

We can write (2.36) in a state-space form as follows:

$$\begin{aligned} \dot{x} &= Ax + B(u + F) \\ y &= Cx \end{aligned} \tag{2.37}$$

where

$$x = \begin{pmatrix} q \\ \dot{q} \end{pmatrix}, \quad A = \begin{pmatrix} 0 & 1 \\ 0 & 0 \end{pmatrix}, \quad B = \begin{pmatrix} 0 \\ \frac{1}{m} \end{pmatrix}, \quad C = \begin{pmatrix} 1 & 0 \end{pmatrix}$$

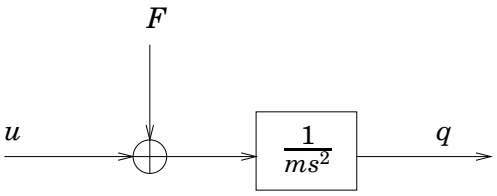


**Figure 2.2** Block diagram of the rigid body.

The parameters $\Lambda$ become (2.8)

$$\begin{cases} \Lambda_2 = \dfrac{1}{a_{12}b} = m \\ \Lambda_1 = \dfrac{K_1 - \mathrm{tr}A}{a_{12}b} = mK_1 \\ \Lambda_0 = \dfrac{K_2 a_{12} - K_1 a_{22} + \det A}{a_{12}b} = mK_2 \end{cases} \tag{2.38}$$

the force observer takes the form (2.15)

$$\begin{cases} \dot{\hat{x}} = A\hat{x} + Bu + K\tilde{x}_1 \\ \tilde{x}_1 = x_1 - \hat{x}_1 \\ \hat{F} = mK_2 \ \tilde{x}_1 \end{cases} \tag{2.39}$$

Stability conditions require $K_1,\ K_2 > 0$. If $K_1^2 > K_2$, then the force estimation error transfer function is SPR. In the simulations (see Figures 2.3-2.5) we chose $K = [6 \ \ 9]^T$ so that both properties are fulfilled. Moreover, looking at (2.27) we can obtain an expression of the poles of $\mathcal{H}(s)$

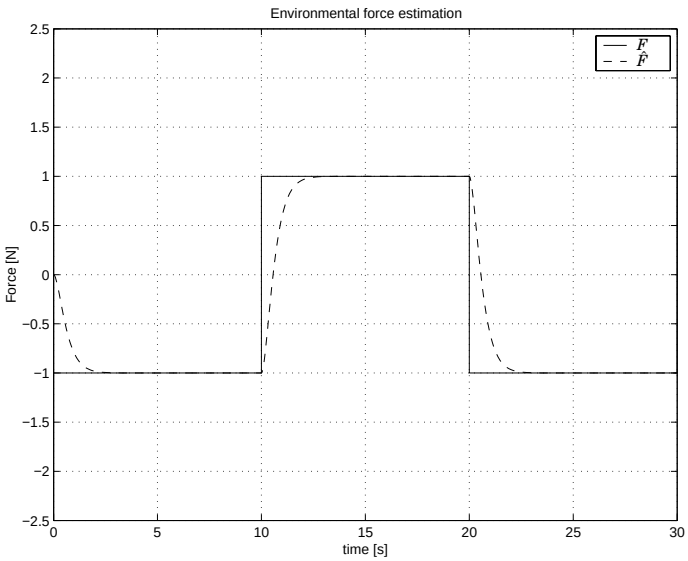


**Figure 2.3** Force estimation in presence of a square environmental force. As we expected, for constant environmental forces, the force estimation error tends to zero.

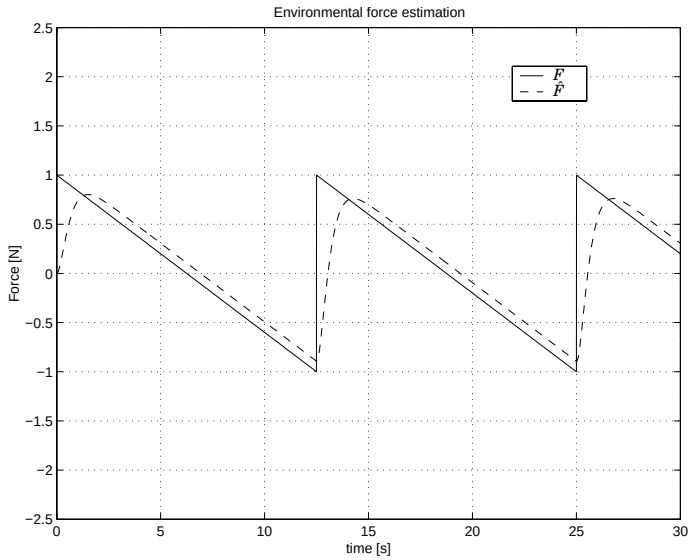


**Figure 2.4** Force estimation and force estimation error in presence of a ramp environmental force. Notice that the force estimation error tends to a constant value. This fact will be exploited later on to build and improved force estimator able to follow ramp signals

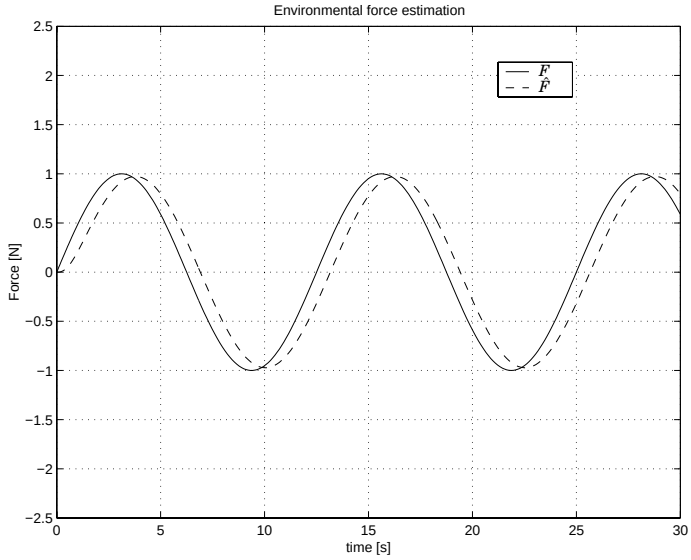


**Figure 2.5** Force estimation in presence of a sinusoidal environmental force. The force estimation error is also a sinusoidal which amplitude and phase lag could have been determined a priori from the bode plots of $\mathcal{H}(s)$ (figure 2.1)

depending on $K_1$ and $K_2$. In the rigid body example, the denominator of $\mathcal{H}(s)$ is $s^2 + K_1 s + K_2$. For instance, for $K_1 = 6$ and $K_2 = 9$, $\mathcal{H}(s)$ has two real poles at $s = -\frac{1}{2}K_1$. Hence, the step response of the force estimator does not present any overshoot or oscillation.

## 2.6 Example II: Damped Rigid Body

Consider the the model of a damped rigid body with mass $m$, damping coefficient $d > 0$, position $q$, input force $u$ and unknown environmental force $F$ as

$$m\ddot{q} + d\dot{q} = u + F \tag{2.40}$$

This can be written in the same form as in (2.37) with

$$x = \begin{pmatrix} q \\ \dot{q} \end{pmatrix}, \quad A = \begin{pmatrix} 0 & 1 \\ 0 & -\frac{d}{m} \end{pmatrix}, \quad B = \begin{pmatrix} 0 \\ \frac{1}{m} \end{pmatrix}, \quad C = \begin{pmatrix} 1 & 0 \end{pmatrix}$$

The parameters $\Lambda$ become (2.8)

$$\begin{cases} \Lambda_2 = \dfrac{1}{a_{12}b} = m \\ \Lambda_1 = \dfrac{K_1 - \mathrm{tr}A}{a_{12}b} = d + mK_1 \\ \Lambda_0 = \dfrac{K_2 a_{12} - K_1 a_{22} + \det A}{a_{12}b} = dK_1 + mK_2 \end{cases} \tag{2.41}$$

and the force observer takes the form (2.15)

$$\begin{cases} \dot{\hat{x}} = A\hat{x} + Bu + K\tilde{x}_1 \\ \tilde{x}_1 = x_1 - \hat{x}_1 \\ \hat{F} = (dK_1 + mK_2)\ \tilde{x}_1 \end{cases} \tag{2.42}$$

The stability condition is $K_1,\ K_2 > 0$. The transfer function $\mathcal{H}(s)$ is SPR for (2.35)

$$K_2 < K_1^2 + \frac{d}{m}K_1 + \frac{d^2}{m^2} \tag{2.43}$$

Simulation results are shown in figure 2.6.

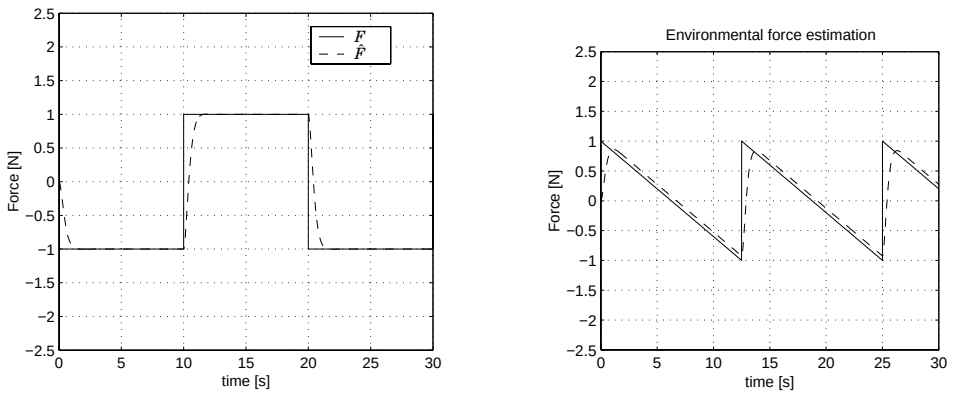


**Figure 2.6** Force estimation with differetn environmental forces in the damped rigid body. The results are almost identical to the rigid body. The observer gains are the same but now a different $\Lambda_0$ was applied.

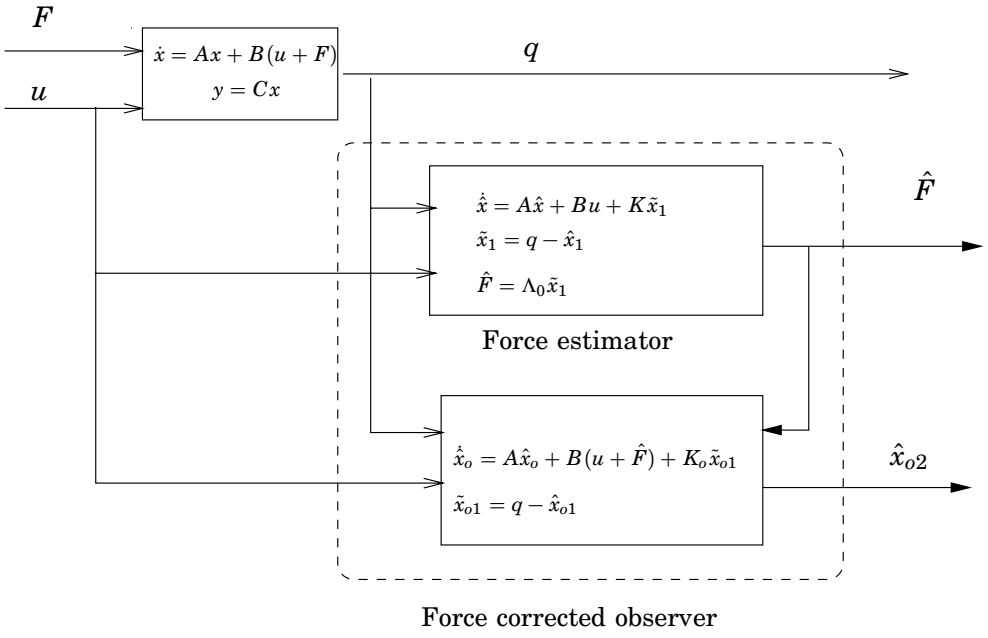


**Figure 2.7** Block diagram of the system and the Force corrected observer.

## 2.7 Force Corrected Observer

Now that we have obtained an estimation of the environmental force we will build an observer that takes into account this force. To avoid confusion, in the future we will call Force observer to (2.15) and reserve the term observer for what is shown in this section. We have assumed that only position measurements are available, and we look forward to obtain an estimate of the system velocities.

An observer copying the system dynamics making use of the previous force estimation can be written

$$\begin{aligned} \dot{\hat{x}}_o &= A\hat{x}_o + B(u + \hat{F}) + K_o(y - \hat{y}_o) \\ \hat{y}_o &= C\hat{x}_o = \hat{x}_{o1} \end{aligned} \tag{2.44}$$

with

$$\hat{x}_o = \begin{pmatrix} \hat{x}_{o1} \\ \hat{x}_{o2} \end{pmatrix}, \quad K_o = \begin{pmatrix} K_{o1} \\ K_{o2} \end{pmatrix} \tag{2.45}$$

We have defined $\hat{x}_o$ as the observer state to differentiate it from the force observer state $\hat{x}$. We can define the observer error as $\tilde{x}_o = x - \hat{x}_o = [\tilde{x}_{o1}, \tilde{x}_{o2}]$. The error dynamics becomes

$$\dot{\tilde{x}}_0 = (A - K_o C)\tilde{x}_o + B\tilde{F} \tag{2.46}$$

Notice that this has the same structure as (2.3) except for that the force $F$ has been replaced by the force estimation error $\tilde{F}$. This fact will be exploited later to build a force observer able to follow ramp environmental forces. The force corrected observer and force observer scheme is illustrated in Figure 2.7. Simulations show the good performance of the observer for enough slow time-varying environmental forces (Figure 2.8). The following parameters have been used in the simulations: $m = 1$ [Kg], $K = K_o = [6\ 9]^T$.

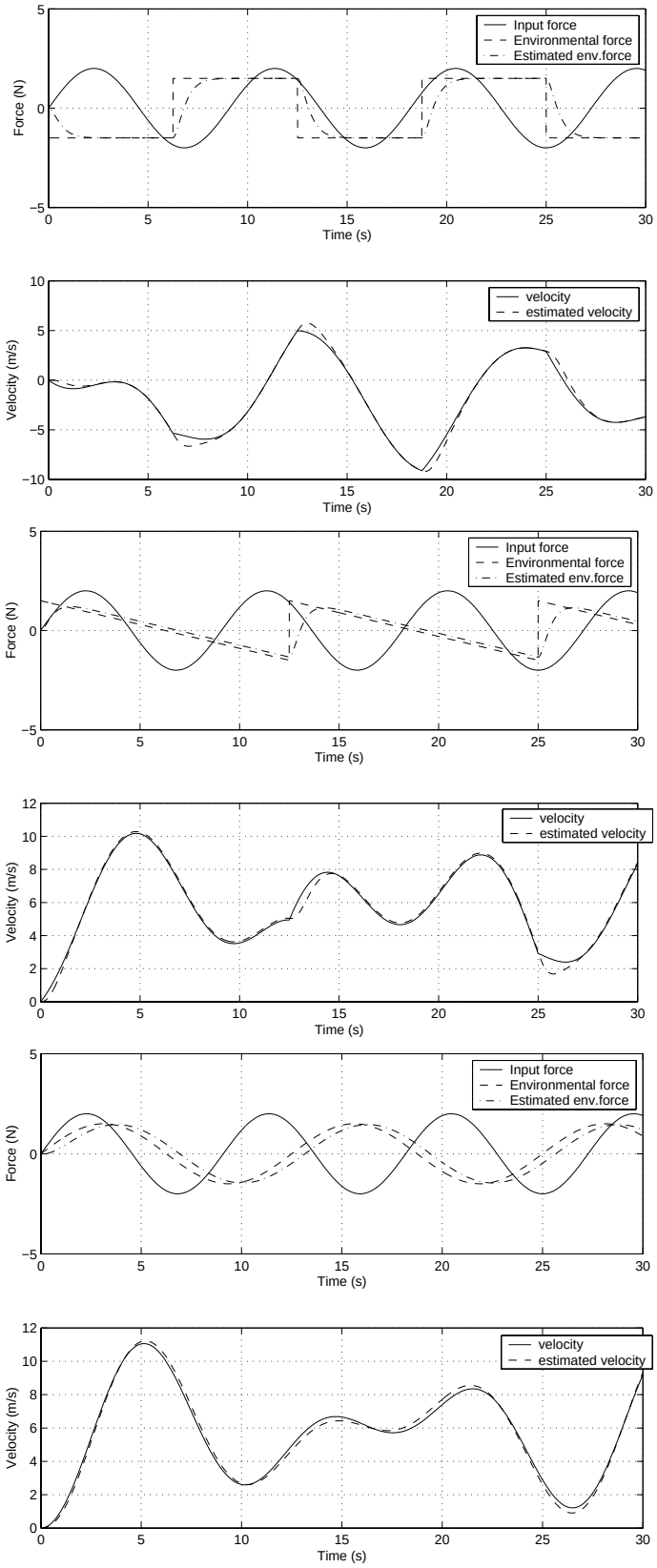


**Figure 2.8** Velocity estimation for the rigid body using the force corrected observer with different environmental forces.

## 2.8 Choice of the Gain $K$

The gain $K = [K_1 \ K_2]^T$ is extremely important and determines the performance of the force estimator. We saw how the constants $\Lambda_2, \ldots, \Lambda_0$ are the coefficients of an imaginary damped spring mass system that guides the position estimation error. These $\Lambda$ parameters are determined by the system matrices $A, B, C$ and the observer gains $K_1,\ K_2$ (2.8). To achieve good force estimations the environmental force should be big enough to deflect over the noise level of the system. A very stiff, heavily damped, spring will not deflect significantly over the influence of small forces and will require very high resolution in the position sensing. We should notice that noise considerations are specially important in our case due to the high pass characteristic of $\mathcal{H}(s)$.

There are different approaches to set this gain.

### Pole Placement

As we can see from (2.27) the poles of $\mathcal{H}(s)$ are the roots of $\Lambda_2 s^2 + \Lambda_1 s + \Lambda_0$. Choosing appropriate gains $K_1$ and $K_2$ and according to (2.8) we can place these poles. For example, it can be interesting to set $K$ such that both poles are real, and avoid overshoots in the step response of the force estimation error.

### Kalman Filter Solution

Having some information about the system noise characteristics it is possible to find an optimal filter that minimizes the variance of the output estimation error. In our case this is directly related to minimize the variance of the force estimation error. We will present the time-invariant continuous version of the *Kalman Filter* found in [18]. Extensive literature can be found on optimal filtering, see for example [19], [20] or [21].

Consider a system

$$\begin{aligned} \dot{x}(t) &= Ax(t) + Bu(t) + v(t) \\ y(t) &= Cx(t) + w(t) \end{aligned} \tag{2.47}$$

with A,B,C constant matrices and

$$\begin{aligned} E[v(t)v'(\tau)] &= Q(t)\delta(t-\tau); \quad E[v(t)] = 0 \\ E[w(t)w'(\tau)] &= R(t)\delta(t-\tau); \quad E[w(t)] = 0 \\ E[v(t)w'(\tau)] &= S(t)\delta(t-\tau) = 0; \quad \text{for all } t \text{ and } \tau \end{aligned} \tag{2.48}$$

Suppose that the noise processes $v$ and $w$ are white, Gaussian, zero mean, and independent with constant covariance matrices $Q$ and $R$. Assume that $R$ is not singular and that the pair $[A, C]$ is detectable.

There exist a time-invariant optimal estimator for the system (2.47) as

$$\dot{\hat{x}} = A\hat{x} + Bu + K(y - C\hat{x}) \tag{2.49}$$

with the constant gain $K$ given by

$$K = PC^T R^{-1} \tag{2.50}$$

and the constant matrix $P$ computed as the solution of the quadratic matrix equation

$$PA^T + AP - PC^T R^{-1} CP + Q = 0 \tag{2.51}$$

Notice that in (2.47) the environmental force is not considered. The observer gain is chosen to minimize the estimation error variance due to the system noises, but not the variance due to the environmental forces. This is a good solution but can be not optimal. There might be a better solution to the choice of $K$ in which a optimization problem considering the force $F$ is solved. However, we must remember that we don't want to minimize the observer error variance but to minimize the force estimation error variance. How this two terms are related and how to solve the optimization problem is an open question that we will not further study.

# 3. Force Observer for Ramp Environmental Forces

## 3.1 Introduction

In this chapter we are going to present a force observer able to follow ramp environmental forces. When exciting the force observer of (2.15) with a ramp environmental force, the force estimation error converged to a non zero value (see Figure 2.4). In this case, if we use the force corrected observer, the position observation error will not converge to zero but to a certain value. The main idea is to characterize this error and use it to build an improved force observer.

## 3.2 New Force Observer

Consider the force corrected observer with error dynamics as in (2.46). Following the same methodology we used to derive the force observer, we will write the observer position estimation error as a function of the force estimation error. We can split (2.46) into

$$\dot{\tilde{x}}_{o1} = a_{11}\tilde{x}_{o1} + a_{12}\tilde{x}_{o2} - K_{o1}\tilde{x}_{o1} \tag{3.1}$$

$$\dot{\tilde{x}}_{o2} = a_{21}\tilde{x}_{o1} + a_{22}\tilde{x}_{o2} + bF - K_{o2}\tilde{x}_{o1} \tag{3.2}$$

from (3.1) is obvious that

$$\tilde{x}_{o2} = \frac{1}{a_{12}}(\dot{\tilde{x}}_{o1} - a_{11}\tilde{x}_{o1} + K_{o1}\tilde{x}_{o1}) \tag{3.3}$$

Deriving (3.1) and using (3.2)-(3.3) we can obtain the equation for the dynamics of $\tilde{x}_{o1}$

$$\Delta_2 \, \dddot{\tilde{x}}_{o1} + \Delta_1 \, \ddot{\tilde{x}}_{o1} + \Delta_0 \, \dot{\tilde{x}}_{o1} = \dot{\tilde{F}} \tag{3.4}$$

with

$$\begin{cases} \Delta_2 = \dfrac{1}{a_{12}b} \\ \Delta_1 = \dfrac{K_{o1} - \mathrm{tr}A}{a_{12}b} \\ \Delta_0 = \dfrac{K_{o2}a_{12} - K_{o1}a_{22} + \det A}{a_{12}b} \end{cases} \tag{3.5}$$

We see from (3.4) that the position estimation error of the force corrected observer $\tilde{x}_{o1}$ behaves as a spring-mass system driven by the force estimation error $\tilde{F}$. The main motivation for this ramp environmental force observer is the fact that when using the force observer of (2.15) with ramp

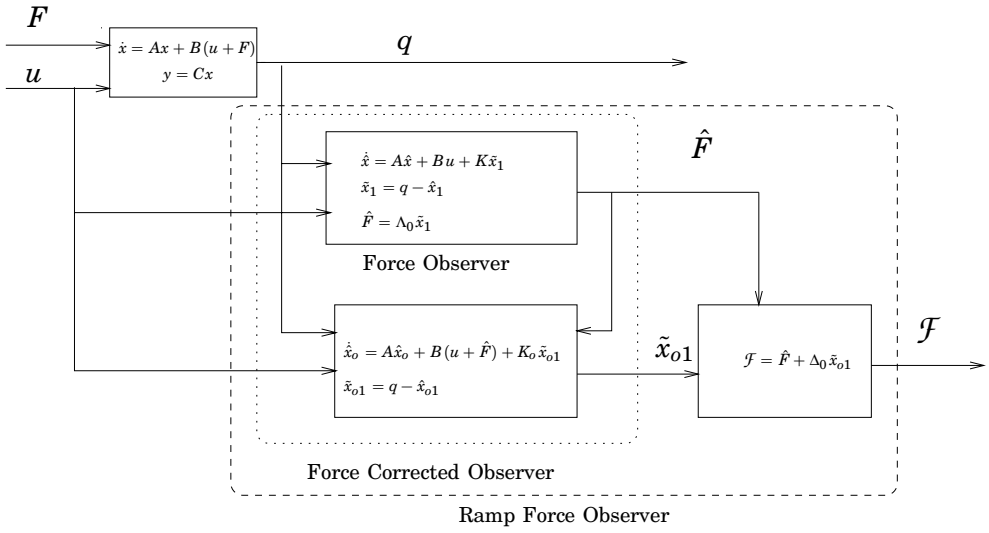


**Figure 3.1** Block diagram of the system and the Ramp Force observer.

environmental forces, the force estimation error $\tilde{F}$ converged to a constant value. Under this situation we expect (3.4) to have an equilibrium point at $\tilde{x}_{o1} = \Delta_0^{-1}\tilde{F}$. Hence, we can obtain an estimation of the force estimation error $\hat{\tilde{F}}$ with

$$\hat{\tilde{F}} = \Delta_0\tilde{x}_{o1} \tag{3.6}$$

The new force estimation will be the sum of the previous force estimation $\hat{F}$ and the estimate of the force estimation error $\hat{\tilde{F}}$

$$\boxed{\mathcal{F} = \hat{F} + \hat{\tilde{F}} = \Lambda_0\tilde{x}_1 + \Delta_0\tilde{x}_{o1}} \tag{3.7}$$

**Summary**

Given a linear system with the structure of (2.1) we can obtain a force estimator $\mathcal{F}$ able to follow ramp environmental forces by using

$$\begin{cases} \dot{\hat{x}} = A\hat{x} + Bu + K\tilde{x}_1 \\ \tilde{x}_1 = x_1 - \hat{x}_1 \\ \hat{F} = \Lambda_0\ \tilde{x}_1 \\ \dot{\hat{x}}_o = A\hat{x}_0 + B(u + F) + K_o\tilde{x}_{o1} \\ \tilde{x}_{o1} = x_1 - \hat{x}_{o1} \\ \mathcal{F} = \hat{F} + \Delta_0\tilde{x}_{o1} \end{cases} \tag{3.8}$$

with $\hat{x} = [\hat{x}_1\ \hat{x}_2]^T$, $\hat{x}_o = [\hat{x}_{o1}\ \hat{x}_{o2}]^T$ $\Lambda_0$ as in (2.8), $\Delta_0$ as in (3.5), $K = [K_1\ K_2]^T$ and $K_o = [K_{o1}\ K_{o2}]^T$.

## 3.3 New Force Estimation Error

The new force estimation error becomes

$$\tilde{\mathcal{F}} = F - \mathcal{F} = \Lambda_2\dddot{\tilde{x}}_1 + \Lambda_1\ddot{\tilde{x}}_1 - \Delta_0\tilde{x}_{o1} \tag{3.9}$$

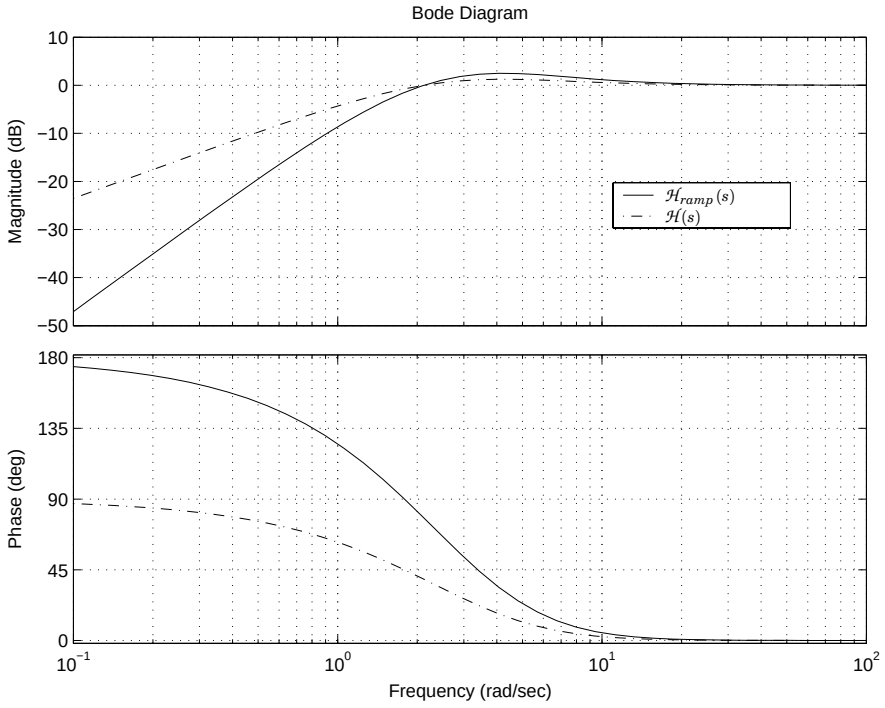


**Figure 3.2** Bode plots of the force estimation error transfer functions $\mathcal{H}$ and $\mathcal{H}_{ramp}$. The observer gains are $K_1 = K_{o1} = 6$ and $K_2 = K_{o2} = 9$.

It is possible to find the new transfer function from the environmental force to the new force estimation error using the following equations:

$$\tilde{F}(s) = \frac{\Lambda_2 s^2 + \Lambda_1 s}{\Lambda_2 s^2 + \Lambda_1 s + \Lambda_0} F(s) \tag{3.10}$$

$$\tilde{x}_{o1}(s) = \frac{1}{\Delta_2 s^2 + \Delta_1 s + \Delta_0} \tilde{F}(s) \tag{3.11}$$

$$\tilde{x}_1(s) = \frac{1}{\Lambda_2 s^2 + \Lambda_1 s + \Lambda_0} F(s) \tag{3.12}$$

and finally we obtain:

$$\mathcal{H}_{ramp}(s) = \frac{\tilde{\mathcal{F}}(s)}{F(s)} = \frac{s^2(\Lambda_2 s + \Lambda_1)(\Delta_2 s + \Delta_1)}{(\Lambda_2 s^2 + \Lambda_1 s + \Lambda_0)(\Delta_2 s^2 + \Delta_1 s + \Delta_0)} \tag{3.13}$$

The new transfer function is strictly stable for all $\Lambda_2, \ldots, \Lambda_0, \Delta_2, \ldots, \Delta_0 > 0$ and has two zeros at $s = 0$. Hence the new force estimation error will tend to zero for constant and ramp signals.

Now we have improved the behavior of the force estimation in front of ramp environmental forces, but as can be seen in the simulations (Fig.3.3) the step response of the system is slower and presents an overshoot. Another interesting characteristic of the new transfer function is the existence of a small peak due to the slow zeros of the system. This means that for certain frequencies there is an amplification of the force estimation error. All this drawbacks can be minimized by choosing the proper observer gains. However, we should always have in mind that increasing these gains

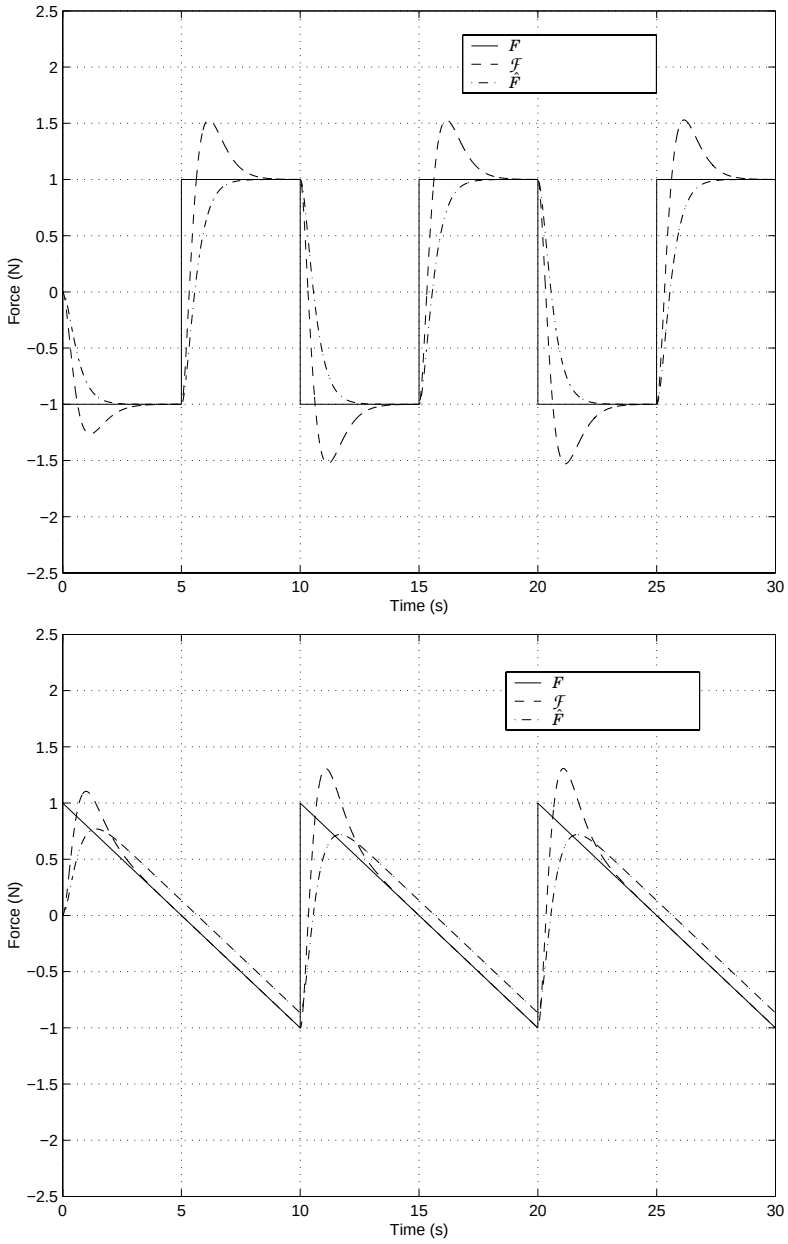


**Figure 3.3** Plots of the force estimations $\mathcal{F}$ and $\hat{F}$ when exciting a rigid body with square and sawtooth environmental forces.

will increase as well the noise sensitivity of the system. This is specially important in our case due to the high pass characteristic of the transfer function. Thus, as usual, there must be a balance between the estimation performance and its robustness against noise.

# 4. Force Observer in Ship Dynamics

## 4.1 Introduction

In this chapter we will introduce an observer for the environmental forces acting on a ship. In the previous chapters we have studied a force observer for linear systems. However a ship is a nonlinear system and a new solution has to be considered. The basic nonlinearity is due to the existence of two reference frames that are expressed through a nonlinear Jacobian matrix. There are many more nonlinear phenomena involved in the ship dynamics, as for instance nonlinear damping forces, that we will not consider, as they can be simplified under certain assumptions. The force estimator deduced here is specially indicated for constant and very slow time varying environmental forces, for instance wind and sea currents.

For detailed understanding of marine vehicles modeling and control see [5], [6], [7], [8].

## 4.2 Ship Model and Problem Formulation

The earth-fixed positions $(x, y)$ and the yaw angle $\psi$ can be expressed in vector form by $\eta = [x, y, \psi]^T$. The ship-fixed velocities can be expressed in vector form by $\nu = [u, v, r]^T$, where $u$ is the surge velocity, $v$ is the sway velocity and $r$ is the yaw angular velocity. Let $\tau = [\tau_u, \tau_v, \tau_r]^T$, expressed in the ship-fixed reference, be the vector of control forces and moments provided by the propulsion system. Let $b = [b_x, b_y, b_\psi]^T$ be the vector of unknown environmental forces and moments acting on the ship expressed in the earth-fixed reference. In Dynamic Positioning systems and Low Speed applications a simplified model of the ship dynamics can be expressed by

$$M\dot{\nu} + D\nu = \tau + J^T(\eta)b \tag{4.1}$$

$$\dot{\eta} = J(\eta)\nu \tag{4.2}$$

The matrix $J(\eta)$ represents the transformation between the ship-fixed reference $XYZ$ and the earth-fixed reference $X_E Y_E Z_E$ and is defined as

$$J(\eta) = J(\psi) = \begin{bmatrix} \cos(\psi) & -\sin(\psi) & 0 \\ \sin(\psi) & \cos(\psi) & 0 \\ 0 & 0 & 1 \end{bmatrix} \qquad \begin{matrix} J^{-1}(\eta) = J^T(\eta) \\ \det J(\eta) = 1 \end{matrix} \tag{4.3}$$

Notice that $J(\eta)$ is non-singular for all $\psi$. The mass matrix $M = M^T$ is *positive definite* and constant. The damping matrix $D$ is in general non-symmetrical but fulfills $x^T Dx = \frac{1}{2}x^T(D + D^T)x > 0$ for all $x \neq 0$, that is

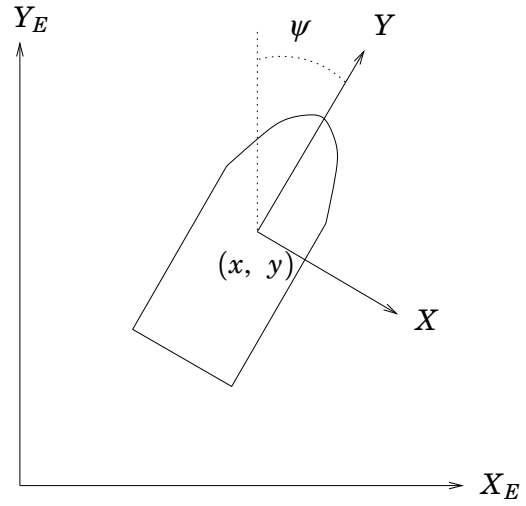


**Figure 4.1** Definition of the earth-fixed $X_E Y_E Z_E$ and ship-fixed $XYZ$ reference frames.

$D$ is *strictly positive*.

$$M = \begin{bmatrix} m_{11} & 0 & 0 \\ 0 & m_{22} & m_{23} \\ 0 & m_{32} & m_{33} \end{bmatrix}, \quad D = \begin{bmatrix} d_{11} & 0 & 0 \\ 0 & d_{22} & d_{23} \\ 0 & d_{32} & d_{33} \end{bmatrix} \tag{4.4}$$

fulfilling

$$0 < M_m < M < M_M, \quad \text{and} \quad 0 < D_m < D < D_M \tag{4.5}$$

## 4.3 Force Observer

We assume that only positions measurements are available, and this is a quite realistic assumption. Velocity sensors in ships are usually based in the vessel surface velocity. This quantity measures the relative velocity between the ship and the water. Under the action of sea currents this measurement is not consistent. The $(x, y)$ position measurements are given by a GPS or a DGPS system. The yaw angle $\psi$ is assumed to be measured with good accuracy by using a gyro compass.

The basic idea is to build a nonlinear observer and use its position estimation error to determine the environmental forces.

Defining $A = -M^{-1}D$ and $B = M^{-1}$ we can rewrite (4.1) and (4.2) as

$$\dot{\nu} = A\nu + B\tau + BJ^T(\eta)b \tag{4.6}$$
$$\dot{\eta} = J(\eta)\nu \tag{4.7}$$

Assuming that only position measurements,$\eta$, are available we can build the following nonlinear observer [6]

$$\dot{\hat{\nu}} = A\hat{\nu} + B\tau + J^T(\eta)K_1\tilde{\eta} \tag{4.8}$$
$$\dot{\hat{\eta}} = J(\eta)\hat{\nu} + K_2\tilde{\eta} \tag{4.9}$$

with $K_1 > 0$ and $K_2 > 0$ constant gain matrices. Defining $\tilde{\eta} = \eta - \hat{\eta}$ and $\tilde{\nu} = \nu - \hat{\nu}$, the observer error dynamics becomes

$$\dot{\tilde{\nu}} = A\tilde{\nu} + BJ^T(\eta)b - J^T(\eta)K_1\tilde{\eta} \tag{4.10}$$
$$\dot{\tilde{\eta}} = J(\eta)\tilde{\nu} - K_2\tilde{\eta} \tag{4.11}$$

From (4.11) it is obvious that

$$\tilde{\nu} = J^T(\eta)(\dot{\tilde{\eta}} + K_2\tilde{\eta}) \tag{4.12}$$

then, deriving (4.11) and using (4.10) and (4.12) we can obtain the equation of the position estimation error dynamics

$$\begin{aligned}\ddot{\tilde{\eta}} \quad &= \dot{J}(\eta)\tilde{\nu} + J(\eta)\dot{\tilde{\nu}} - K_2\dot{\tilde{\eta}} \\ &= \dot{J}(\eta)J^T(\eta)(\dot{\tilde{\eta}} + K_2\tilde{\eta}) \\ &+J(\eta)\Big(A\big(J^T(\eta)(\dot{\tilde{\eta}} + K_2\tilde{\eta})\big) + BJ^T(\eta)b - J^T(\eta)K_1\tilde{\eta}\Big) \\ &-K_2\dot{\tilde{\eta}}\end{aligned} \tag{4.13}$$

Collecting terms it is straight forward to obtain

$$\boxed{\Lambda_2\ddot{\tilde{\eta}} + \Lambda_1\dot{\tilde{\eta}} + \Lambda_0\tilde{\eta} = b} \tag{4.14}$$

with

$$\begin{cases}\Lambda_2 = J(\eta)MJ^T(\eta) \\ \Lambda_1 = J(\eta)MJ^T(\eta)\big[K_2 - \dot{J}(\eta)J^T(\eta) - J(\eta)AJ^T(\eta)\big] \\ \Lambda_0 = J(\eta)MJ^T(\eta)\big[K_1 - \dot{J}(\eta)J^T(\eta)K_2 - J(\eta)AJ^T(\eta)K_2\big]\end{cases} \tag{4.15}$$

The position estimation error behaves like a damped spring mass system driven by the environmental force $b$. This is a similar result to the one obtained when studying the linear case. For constant environmental forces there is an equilibrium for (4.14) that suggests the estimator

$$\boxed{\hat{b} = \Lambda_0\tilde{\eta}} \tag{4.16}$$

The structure of the force estimator is the same as in the linear case, but there are some qualitative differences that have to be considered. The matrices $\Lambda$ are time varying and contain a derivative term of the transformation matrix $\dot{J}(\eta)$ which seems hard to deal with. Lets study this matrices with some detail.

**About the $\Lambda$ Matrices**

Given an $n \times n$ matrix $A$ we denote by $A_m$ and $A_M$, respectively the minimum and maximum eigenvalue of $\frac{1}{2}(A^T + A)$. Consider the matrix norm $\|\cdot\|$ defined as

$$\|A\| = \sqrt{\max_{eigenvalue} A^TA} \tag{4.17}$$

Define

$$\rho = \begin{bmatrix} 0 \\ 0 \\ r \end{bmatrix}, \qquad S(\rho) = \begin{bmatrix} 0 & -r & 0 \\ r & 0 & 0 \\ 0 & 0 & 0 \end{bmatrix} \tag{4.18}$$

where $r$ is the vessel turning rate or yaw velocity. The following interesting properties hold

$$\dot{J}(\eta) = J(\eta)S(\rho) \tag{4.19}$$

$$J(\eta)S(\rho)J^T(\eta) = S(\rho) \tag{4.20}$$

$$\|S(\rho)\| = |r| \tag{4.21}$$

Using (4.19),(4.20) and (4.21) we can derive some valuable information about the matrices $\Lambda$. Remember that we defined $A = -M^{-1}D$ and assumed that all the eigenvalues of $A$ had negative real part. An interesting property that follows shows how the derivative term on $J(\eta)$ can be disregarded under certain assumptions.

PROPERTY 4.1
if the absolute value of the ship turning rate $|r|$ is smaller than a certain boundary $\delta$ and according to (4.19) and (4.21) the derivative term in $\Lambda_0$ fulfills

$$\|\dot{J}(\eta)J^T(\eta)K_2\| \leq |\delta|\|K_2\| \tag{4.22}$$

which means that if $\delta$ is enough small, this term can be disregarded without affecting the quality of the force estimator. □

PROPERTY 4.2—POSITIVENESS OF $\Lambda$ MATRICES
Consider the positive diagonal observer gains $K_1$ and $K_2$. Assume that $|r| < \delta$. If they are chosen such that

$$K_{2m} + \{M^{-1}D\}_m > |\delta| \tag{4.23}$$

$$K_{1m} + \{M^{-1}D\}_m K_{2m} > |\delta|\|K_2\| \tag{4.24}$$

then the matrices $\Lambda$ are *strictly positive*.

$$\begin{aligned} \Lambda_2 \quad &= J(\eta)MJ^T(\eta) \geq M_m > 0 && (4.25) \\ \Lambda_1 \quad &= J(\eta)MJ^T(\eta)\big[K_2 - \dot{J}(\eta)J^T(\eta) - J(\eta)AJ^T(\eta)\big] \\ &= J(\eta)MJ^T(\eta)\big[K_2 - \underbrace{S(\rho)}_{\leq|\delta|} \underbrace{-J(\eta)AJ^T(\eta)}_{\geq\{M^{-1}D\}_m}\big] \\ &\geq M_m\big[K_{2m} - |\delta| + \{M^{-1}D\}_m\big] > 0 && (4.26) \\ \Lambda_0 \quad &= J(\eta)MJ^T(\eta)\big[K_1 - \dot{J}(\eta)J^T(\eta)K_2 - J(\eta)AJ^T(\eta)K_2\big] \\ &= J(\eta)MJ^T(\eta)\big[K_1 - \underbrace{S(\rho)K_2}_{\leq|\delta|\|K_2\|} \underbrace{-J(\eta)AJ^T(\eta)K_2\big]}_{\geq\{M^{-1}D\}_m K_{2m}} \\ &\geq M_m\big[K_{1m} - |\delta|\|K_2\| + \{M^{-1}D\}_m K_{2m}\big] > 0 && (4.27) \end{aligned}$$

□

## 4.4 Stability Analysis

Lets first study the linearized system around the trajectory $\psi = 0$, that is when the ship is moving forward with a constant heading angle equal to zero. In this case we have

$$\begin{cases} J(\eta) = J^T(\eta) = I \\ \Lambda_2 = M > 0 \\ \Lambda_1 = M\big[K_2 - A\big] > 0 \\ \Lambda_0 = M\big[K_1 - AK_2\big] > 0 \end{cases} \tag{4.28}$$

The linearized position estimation error dynamics can be written in state space form

$$\begin{bmatrix} \dot{\tilde{\eta}} \\ \ddot{\tilde{\eta}} \end{bmatrix} = \underbrace{\begin{bmatrix} 0 & I \\ -B\Lambda_0 & -B\Lambda_1 \end{bmatrix}}_{\Phi} \begin{bmatrix} \tilde{\eta} \\ \dot{\tilde{\eta}} \end{bmatrix} + \begin{bmatrix} 0 \\ B \end{bmatrix} b \tag{4.29}$$

with $B\Lambda_0$ and $B\Lambda_1$ *strictly positive* matrices. We will show that the system matrix $\Phi$ is *Hurwitz* so that the linearized error dynamics system is asymptotically stable (see [15, page 192]).

Let $\lambda \in C$ be an eigenvalue of $\Phi$ with corresponding eigenvector $v = (v_1, v_2),\ v \neq 0$. Then,

$$\lambda \begin{bmatrix} v_1 \\ v_2 \end{bmatrix} = \begin{bmatrix} 0 & I \\ -B\Lambda_0 & -B\Lambda_1 \end{bmatrix} \begin{bmatrix} v_1 \\ v_2 \end{bmatrix} = \begin{bmatrix} v_2 \\ -B\Lambda_0 v_1 - B\Lambda_1 v_2 \end{bmatrix} \tag{4.30}$$

It follows that if $\lambda = 0$ then $v = 0$, and hence $\lambda = 0$ is not an eigenvalue of $\Phi$. Further, if $\lambda \neq 0$, then $v_2 = 0$ implies that $v_1 = 0$. Thus, $v_1,\ v_2 \neq 0$ and we may assume without loss of generality that $\|v_1\| = 1$. Using this we write

$$\lambda^2 = v_1^* \lambda^2 v_1 = v_1^* \lambda v_2 \tag{4.31}$$

$$= v_1^*(-B\Lambda_0 v_1 - B\Lambda_1 v_2) = -v_1^* B\Lambda_0 v_1 - \lambda v_1^* B\Lambda_1 v_1 \tag{4.32}$$

where $*$ denotes complex conjugate transpose. Since $\alpha = v_1^* B\Lambda_0 v_1 > 0$ and $\beta = v_1^* B\Lambda_1 v_1 > 0$, we have

$$\lambda^2 + \alpha\lambda + \beta = 0 \qquad \alpha, \beta > 0 \tag{4.33}$$

and hence, the real part of $\lambda$ is negative so that $\Phi$ is *Hurwitz*. This implies that the linearized system is asymptotically stable and we can conclude local asymptotic stability complete nonlinear system. This is a good result, but we still want to know more about the effect of the environmental force in this system. We also need some conditions over the observer gain $K$ that applies to the nonlinear system.

Consider the ship model of (4.6)-(4.7), the nonlinear observer of (4.8)-(4.9) and the observer error dynamics of (4.10)-(4.11).Consider the following Lyapunov function candidate

$$V(\tilde{\eta}, \tilde{\nu}) = \frac{1}{2}(\tilde{\eta}^T P_1 \tilde{\eta} + \tilde{\nu}^T P_2 \tilde{\nu}) \tag{4.34}$$

it's time derivative along the solutions of (4.10) and (4.11) is

$$\begin{aligned}\dot{V} &= \tilde{\eta}^T P_1 \dot{\tilde{\eta}} + \tilde{\nu}^T P_2 \dot{\tilde{\nu}} \\ &= \tilde{\eta}^T P_1 \big[J(\eta)\tilde{\nu} - K_2\tilde{\eta}\big] + \tilde{\nu}^T P_2 \big[A\tilde{\nu} + BJ^T(\eta)b - J^T(\eta)K_1\tilde{\eta}\big] \\ &= -\tilde{\eta}^T \big[P_1 K_2\big]\tilde{\eta} - \tilde{\nu}^T \big[-P_2 A\big]\tilde{\nu} + \tilde{\nu}^T \big[J^T(\eta)P_1^T - P_2 J^T(\eta)K_1\big]\tilde{\eta} \\ &+ \tilde{\nu}^T P_2 B J^T(\eta)b \end{aligned} \tag{4.35}$$

taking $P_1 = I, P_2 = I$ and remembering that $B = M^{-1}, A = -M^{-1}D$ we have

$$\begin{aligned}\dot{V} &= -\tilde{\eta}^T K_2\tilde{\eta} - \tilde{\nu}^T \big[M^{-1}D\big]\tilde{\nu} + \tilde{\nu}^T J^T(\eta)\big[I - K_1\big]\tilde{\eta} \\ &+ \tilde{\nu}^T B J^T(\eta)b \end{aligned} \tag{4.36}$$

we can write

$$\dot{V} \leq -\sigma_1\|\tilde{\eta}\|^2 - \sigma_2\|\tilde{\nu}\|^2 + (1+\sigma_3)\|\tilde{\eta}\|\|\tilde{\nu}\| + \tilde{\nu}^T B J^T(\eta)b \tag{4.37}$$

were

$$\begin{aligned}\sigma_1 &= K_{2_m} > 0 \\ \sigma_2 &= \{M^{-1}D\}_m > 0 \\ \sigma_3 &= \|K_1\| > 0 \end{aligned} \tag{4.38}$$

We defined the observer gain matrices $K_1, K_2$ to be diagonal positive definite so it holds $\sigma_1 > 0$ and $\sigma_3 > 0$. The mass matrix $M$ and the damping matrix $D$ are positive definite matrices. However this does not necessary imply that $A = -M^{-1}D$ is *Hurwitz*, characteristic of course-stable ships. An extension to the design of nonlinear observers of course-unstable ships is done in [9]. To assure $\sigma_2 > 0$ we will assume that $A$ is *Hurwitz*.

Now, as a first approach, let the environmental force $b$ be zero. Then defining $z = \begin{bmatrix}\tilde{\eta} & \tilde{\nu}\end{bmatrix}^T$ we can rewrite (4.37) in the form

$$\dot{V} \leq -z^T Q z \tag{4.39}$$

It can be shown that $Q$ is positive definite if

$$\sigma_1 > \frac{(1+\sigma_3)^2}{4\sigma_2} \tag{4.40}$$

Hence, we have proven global asymptotic stability of the observer when $b = 0$. Consider now a bounded nonzero environmental force. From (4.37) equation (4.39) becomes

$$\begin{aligned}\dot{V} &\leq -z^T Q z + \tilde{\nu}^T B b \\ &= -\underbrace{z^T Q z}_{1} + \underbrace{z^T \begin{bmatrix}0 \\ B\end{bmatrix} b}_{2} \end{aligned} \tag{4.41}$$

When $z$ is big, the first part of (4.41) will be dominant to the second part due to the quadratic term in $z$ so $\dot{V}$ will be negative. On the other hand,

when $z$ is small the second term will be more important so $\dot{V}$ will become positive. This suggests that the Lyapunov function $V$ remains bounded and so does the observer estimation error.

The system shows an interesting passivity property. Integrating (4.41) over [0 $t$] we have

$$V(t) - V(0) \leq -\int_0^t z^T(\tau) Q z(\tau) \mathrm{d}\tau + \int_0^t z^T \begin{bmatrix} 0 \\ B \end{bmatrix} b \mathrm{d}\tau \tag{4.42}$$

$$\leq \int_0^t z^T \begin{bmatrix} 0 \\ B \end{bmatrix} b \mathrm{d}\tau \tag{4.43}$$

which shows that the system is passive with respect to the input $b$ and output $(0 \quad B^T)z = B^T\tilde{\nu}$ with storage function $V$ and dissipative rate $z^T Q z$.

## 4.5 Simulation Results

The ship model used in the simulations is taken from [7], in which the $M$ and $D$ matrices are

$$M = \begin{bmatrix} 5.3122 \cdot 10^6 & 0 & 0 \\ 0 & 8.2831 \cdot 10^6 & 0 \\ 0 & 0 & 3.7454 \cdot 10^9 \end{bmatrix} \tag{4.44}$$

$$D = \begin{bmatrix} 5.0242 \cdot 10^4 & 0 & 0 \\ 0 & 2.7229 \cdot 10^5 & -4.3933 \cdot 10^6 \\ 0 & -4.3933 \cdot 10^6 & 4.1894 \cdot 10^8 \end{bmatrix} \tag{4.45}$$

The observer gains have been chosen

$$K_1 = \begin{bmatrix} 0.1 & 0 & 0 \\ 0 & 0.1 & 0 \\ 0 & 0 & 0.1 \end{bmatrix}, \quad K_2 = \begin{bmatrix} 1.1 & 0 & 0 \\ 0 & 1.1 & 0 \\ 0 & 0 & 1.1 \end{bmatrix} \tag{4.46}$$

The input signal was a constant surge force of value $1 \cdot 10^5$ $N$. The environmental forces were designed to simulate the wind and sea disturbances characteristics. We used a second order system excited by a white-noise sequence, see [5] for details.

Simulation results are shown in Figures 4.2-4.7.

## 4.6 Discussion

The input signal was constant surge force and no control strategy was implemented so the environmental forces could modify very easily the heading angle of the vessel. This is not a real situation as in most of the times there will be a control signal that will try to compensate for these disturbances. In this situation, constant heading angle, simulations proved a better behaviour of the Force Observer.

We assumed than only position measurements will be used. However, the matrice $\Lambda_0$ contain a derivative term of $J(\eta)$ that implies the use of

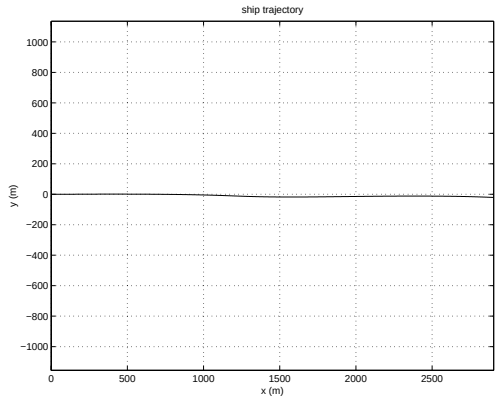


**Figure 4.2** Ship trajectory during the simulations.

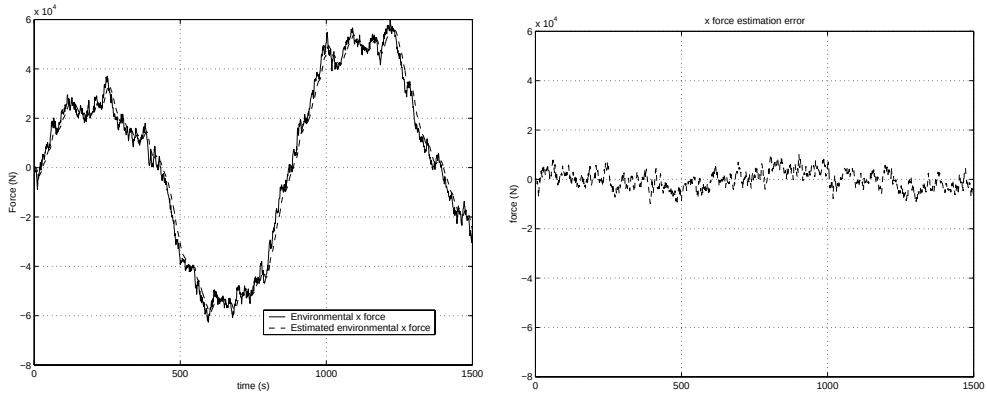


**Figure 4.3** Estimation of the $x$ environmental force $\hat{b}_x$ and force estimation error

the yaw velocity $r$. Thanks to Property (4.1) we see how this term can be disregarded. Actually, in all the simulations $\Lambda_0$ has been computed without considereing the derivative term, that is

$$\hat{\Lambda}_0 = J(\eta)MJ^T(\eta)\big[K_1 - J(\eta)AJ^T(\eta)K_2\big] \tag{4.47}$$

Simulations showed how this simplification did not affect the the force estimation.

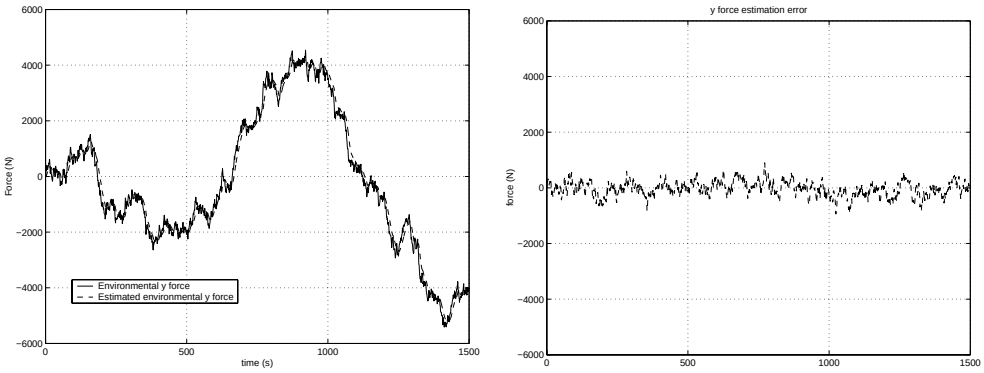


**Figure 4.4** Estimation of the $y$ environmental force $\hat{b}_y$ and force estimation error

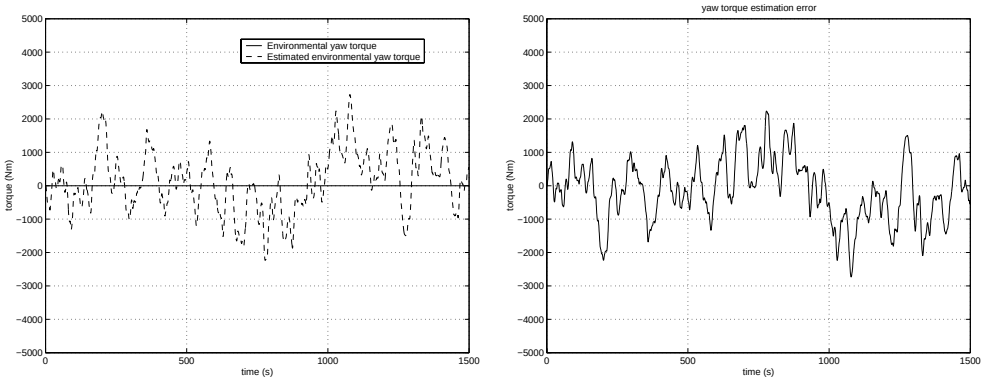


**Figure 4.5** Estimation of the $yaw$ environmental force $\hat{b}_\psi$ and force estimation error

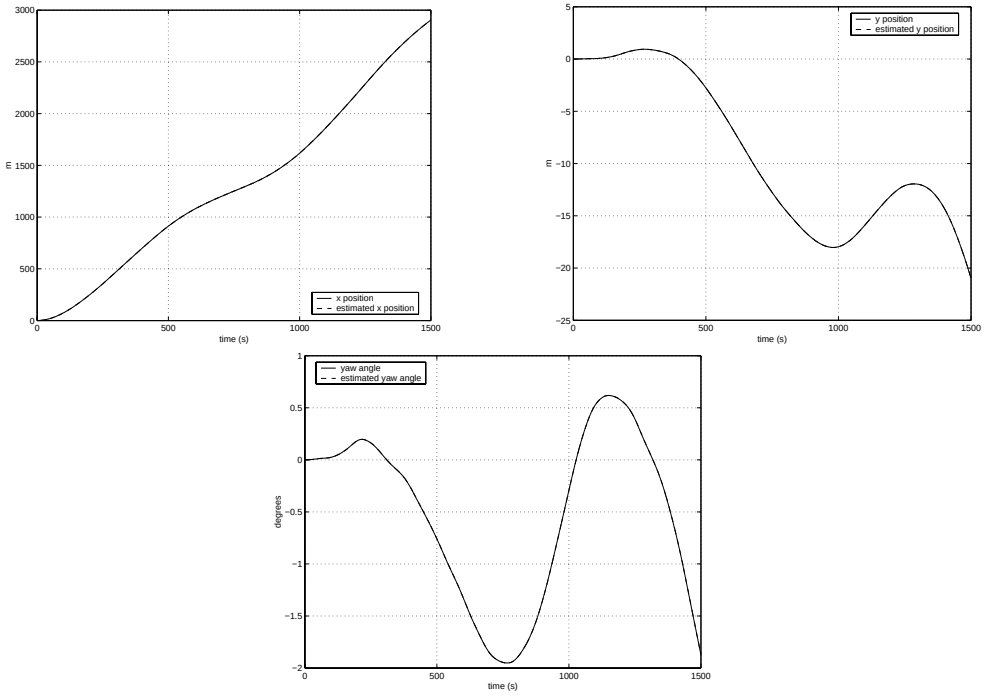


**Figure 4.6** Ship position and position estimation $\eta = [x, y, \psi]$ and $\hat{\eta}$.

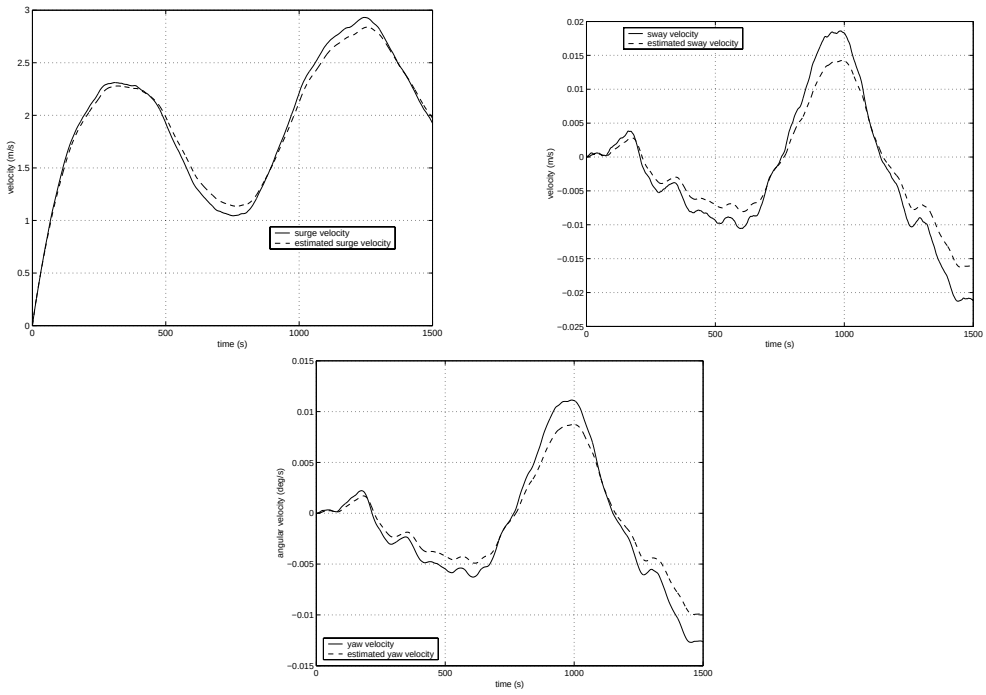


**Figure 4.7** Ship velocity and velocity estimation $\nu = [u, v, r]$ and $\hat{\nu}$.

# 5. Force Observer for Robot Manipulators

## 5.1 Introduction

In this chapter we will introduce an observer for the environmental forces acting on a robot manipulator. Robotic applications often imply the interaction of the manipulator with its environment, which generates contact forces of extremely importance for the task performance. Force control applications in robotics are more common every day, and its theoretical knowledge is far ahead of the practical implementation of these methods. The main reason for this is the unpopularity of force sensors, due to their high prize and complexity.

We present a model based approach to the estimation of these environmental forces. We assume that only position measurements are available and, again, this is a real situation in most of the industrial robotic manipulators.

## 5.2 System Model and Properties

The equations of motion of a robot manipulator can be written as

$$M(q)\ddot{q} + C(q,\dot{q})\dot{q} + D\dot{q} + G(q) = u + J^T(q)F \tag{5.1}$$

where

| | | |
|---|---|---|
| $q$ | vector of generalized coordinates | $q \in R^n$ |
| $\dot{q}$ | vector of generalized velocities | $\dot{q} \in R^n$ |
| $M(q)$ | inertia matrix | $M(q) \in R^{n\times n}$ |
| $C(q,\dot{q})\dot{q}$ | matrix of centrifugal and Coriolis torques | $C(q,\dot{q})\dot{q} \in R^{n\times n}$ |
| $D$ | diagonal matrix of viscous friction coefficients | $D \in R^{n\times n}$ |
| $G(q)$ | vector of gravitational torques | $G(q) \in R^n$ |
| $u$ | vector of input torques | $u \in R^n$ |
| $J(q)$ | geometric Jacobian matrix | $J(q) \in R^{n\times l}$ |
| $F$ | wrench of environmental forces and torques | $F \in R^l$ |

The vector of environmental forces and torques $F$ is unknown and needs to be estimated. $F$ is acting on the manipulator end-effector and is transmitted to the joint torques through the transpose of the Jacobian $J(q)$.

The robot model has the following important properties

PROPERTY 5.1
$M(q)$ is a symmetric positive definite matrix fulfilling

$$0 < M_m < \|M(q)\| < M_M \qquad \forall\ q \in R^n \tag{5.2}$$

□

PROPERTY 5.2
A suitable definition of $C(q,\dot{q})$ makes the matrix $\dot{M}(q) - 2C(q,\dot{q})$ skew-symmetric. Remember that if $A$ is a $n \times n$ skew-symmetric matrix then for all $x \in R^n$, $x^T A x = 0$. □

PROPERTY 5.3
Given two $n \times 1$ vectors x and y

$$C(q,x)y = C(q,y)x \tag{5.3}$$

□

PROPERTY 5.4
The norm of $C(q,\dot{q})$ satisfies

$$\|C(q,\dot{q})\| \leq k_c \|\dot{q}\| \tag{5.4}$$

□

We will assume in the future that the robot velocities are bounded so that

$$\|\dot{q}(t)\| \leq k_q, \quad \forall t \geq 0 \tag{5.5}$$

## 5.3 Force Observer

The basic idea is to build a nonlinear observer for the system, as the one presented in [2], and use its position estimation errors to deduce the environmental force. Defining the states $x_1 = q$ and $x_2 = \dot{q}$ we can write a state space representation of (5.1) as

$$\dot{x}_1 = x_2 \tag{5.6}$$

$$\dot{x}_2 = M^{-1}(x_1)\big[ - C(x_1,\dot{x}_1)\dot{x}_1 - D\dot{x}_1 - G(x_1) + u + J^T(x_1)F\big] \tag{5.7}$$

We can construct a nonlinear observer copying the dynamics of the system, without considering the environmental force. We assume that only joint positions are measured so that $x_1$ is the output variable.

$$\dot{\hat{x}}_1 = \hat{x}_2 + K_1\tilde{x}_1 \tag{5.8}$$

$$\dot{\hat{x}}_2 = M^{-1}(x_1)\big[ - C(x_1,\dot{\hat{x}}_1)\dot{\hat{x}}_1 - D\dot{\hat{x}}_1 - G(x_1) + u + K_2\tilde{x}_1\big] \tag{5.9}$$

$$\tilde{x}_1 = x_1 - \hat{x}_1 = q - \hat{x}_1 \tag{5.10}$$

where $K_1$ and $K_2$ are symmetric positive definite gain matrices, usually diagonal. Subtracting (5.9) from (5.6) we obtain

$$\dot{\tilde{x}}_1 = \tilde{x}_2 - K_1\tilde{x}_1 \tag{5.11}$$

$$\begin{aligned}\dot{\tilde{x}}_2 &= M^{-1}\big[ - C(x_1,\dot{x}_1)\dot{x}_1 - C(x_1,\dot{\hat{x}}_1)\dot{\hat{x}}_1 - D\dot{\tilde{x}}_1 + J^T(x_1)F \\ &\quad - K_2\tilde{x}_1\big] \\ &= M^{-1}\big[ - C(x_1,\dot{x}_1)\dot{\tilde{x}}_1 - C(x_1,\dot{\hat{x}}_1)\dot{\hat{x}}_1 - D\dot{\tilde{x}}_1 + J^T(x_1)F \\ &\quad - K_2\tilde{x}_1\big]\end{aligned} \tag{5.12}$$

where property 5.3 has been used. Now it is possible to find the dynamics for $\tilde{x}_1$ by differentiating (5.11) and using (5.12)

$$\begin{aligned}\ddot{\tilde{x}}_1 &= \dot{\hat{x}}_2 - K_1\dot{\tilde{x}}_1 \\ &= M^{-1}\big[-C(x_1,\dot{x}_1)\dot{\tilde{x}}_1 - C(x_1,\dot{\hat{x}}_1)\dot{\tilde{x}}_1 - D\dot{\tilde{x}}_1 + J^T(x_1)F - K_2\tilde{x}_1\big] \\ &\quad - K_1\dot{\tilde{x}}_1\end{aligned} \tag{5.13}$$

Then collecting terms it is straight forward to find

$$\boxed{\Lambda_2\ddot{\tilde{x}}_1 + \Lambda_1\dot{\tilde{x}}_1 + \Lambda_0\tilde{x}_1 = J^T(x_1)F} \tag{5.14}$$

with

$$\begin{cases}\Lambda_2 = M(x_1) \\ \Lambda_1 = C(x_1,\dot{x}_1) + C(x_1,\dot{\hat{x}}_1) + D + M(x_1)K_1 \\ \Lambda_0 = K_2\end{cases} \tag{5.15}$$

Again, the observer position estimation error behaves as a damped spring mass system driven by the environmental force. The force $F$ is defined in the cartesian space, and the term $J^T(x_1)F$ shows how this environmental force is transmitted to the joint space through the transpose of the geometric Jacobian. We expect (5.14) to have an equilibrium point that suggests the force estimator

$$\boxed{\hat{F} = J^{T^\dagger}(x_1)\Lambda_0\tilde{x}_1} \tag{5.16}$$

with † denoting the matrix *pseudo-inverse* defined as $A^\dagger = (A^TA)^{-1}A^T$.

PROPERTY 5.1—POSITIVENESS OF $\Lambda$ MATRICES
If the observer gain $K_1$ is chosen such that

$$K_{1m} > \frac{2k_ck_q - D_m}{M_m} \tag{5.17}$$

then the $\Lambda$ matrices are *strictly positive*. we see that

$$\Lambda_2 \geq M_m > 0 \tag{5.18}$$

$$\Lambda_1 = \underbrace{C(x_1,\dot{x}_1) + C(x_1,\dot{\hat{x}}_1)}_{\geq -2k_ck_q} + \underbrace{D + M(x_1)K_1}_{\geq D_m + M_mK_{1m}} > 0 \tag{5.19}$$

$$\Lambda_0 \geq K_{2m} > 0 \tag{5.20}$$

□

As we will see later the positiveness of the $\Lambda$ matrices assured by (5.17) is closely related to the stability of the observer.

## 5.4 Stability Analysis

We first need to show the stability of the previous nonlinear observer in the case of zero environmental forces. Then we will study what happens when this force is not zero and show consistency of the proposed force estimator.

Let $z^T = [\tilde{x}_1^T \quad \dot{\tilde{x}}_1^T]$ and let $H(x_1) = \text{block diag}\big[K_2,\ M(x_1)\big]$. Consider the following Lyapunov function candidate

$$V(z,t) = \frac{1}{2} z^T H(x_1) z \tag{5.21}$$

its time derivative along the solutions of (5.14) is

$$\begin{aligned} \dot{V}(z,t) &= \dot{\tilde{x}}_1^T K_2 \tilde{x}_1 + \dot{\tilde{x}}_1^T M(x_1) \ddot{\tilde{x}}_1 + \frac{1}{2} \dot{\tilde{x}}_1^T \dot{M}(x_1) \dot{\tilde{x}}_1 \\ &= \dot{\tilde{x}}_1^T \big[ - C(x_1, \dot{x}_1)\dot{\tilde{x}}_1 - C(x_1, \dot{\hat{x}}_1)\dot{\tilde{x}}_1 - D\dot{\tilde{x}}_1 + J^T(x_1)F - K_2 \dot{\tilde{x}}_1 \\ &\quad - M(x_1) K_1 \dot{\tilde{x}}_1 \big] + \dot{\tilde{x}}_1 K_2 \tilde{x}_1 + \frac{1}{2} \dot{\tilde{x}}_1^T \dot{M}(x_1) \dot{\tilde{x}}_1 \end{aligned} \tag{5.22}$$

Simplifying and using property 5.2 we have

$$\begin{aligned} \dot{V}(z,t) = -\dot{\tilde{x}}_1^T \big[ M(x_1) K_1 + D \big] \dot{\tilde{x}}_1 - \dot{\tilde{x}}_1^T C(x_1, \dot{\hat{x}}_1) \dot{\tilde{x}}_1 \\ + \dot{\tilde{x}}_1^T J^T(x_1) F \end{aligned} \tag{5.23}$$

properties 5.3 and 5.4 imply

$$\begin{aligned} |\dot{\tilde{x}}_1^T C(x_1, \dot{\hat{x}}_1) \dot{\tilde{x}}_1| &= |\dot{\tilde{x}}_1^T C(x_1, \dot{x}_1) \dot{\tilde{x}}_1 + \dot{\tilde{x}}_1^T C(x_1, \dot{\hat{x}}_1) \dot{\tilde{x}}_1| \\ &\leq \|\dot{\tilde{x}}_1\|^2 k_c (\|\dot{\tilde{x}}_1\|^2 + k_q) \end{aligned} \tag{5.24}$$

then

$$\dot{V} \leq -\|\dot{\tilde{x}}_1\|^2 \big[ M_m K_{1m} + D_m - k_c (\|\dot{\tilde{x}}_1\|^2 + k_q) \big] + \dot{\tilde{x}}_1^T J^T(x_1) F \tag{5.25}$$

Hence, if

$$\|\dot{\tilde{x}}_1\|^2 \leq \frac{M_m K_{1m} + D_m}{k_c} - k_q \tag{5.26}$$

and

$$K_{1m} > \frac{k_q k_c - D_m}{M_m} \tag{5.27}$$

so that the right side of (5.26) is positive, we have

$$\dot{V} \leq -\beta \|\dot{\tilde{x}}_1\|^2 + \dot{\tilde{x}}_1^T J^T(x_1) F \tag{5.28}$$

where $\beta$ is a positive constant. Moreover

$$\frac{1}{2} H_m \|z\|^2 \leq V(z,t) \leq \frac{1}{2} H_M \|z\|^2 \tag{5.29}$$

Lets first assume that the environmental force $F$ is zero. From (5.29) We see that $V(z,t)$ is a positive definite decrescent function. Furthermore, $\dot{V}$ is a negative semi-definite function for all $z$ fulfilling (5.26) under assumption (5.27). Hence, we conclude that in this case the point $z = 0$ is uniformly stable [23, p. 107].

Now consider a nonzero environmental force $F$. Integrating equation (5.28) over [0 $t$] we have

$$V(t) - V(0) \leq \int_0^t \beta \|\dot{\tilde{x}}_1(s)\|^2 \mathrm{d}s + \int_0^t \dot{\tilde{x}}_1^T(s) J^T(x_1) F(s) \mathrm{d}s \tag{5.30}$$

Then, if equations (5.26) and (5.27) are fulfilled, the system in (5.14) is passive with input $J^T(x_1)F$, output $\dot{\tilde{x}}_1$, storage function $V$ and dissipation rate $\beta \|\dot{\tilde{x}}_1\|^2$.

# 6. Force Estimation Experiment: Robotic Manipulator

## 6.1 Introduction

In this chapter we will present an experiment in which the force observer will be tested in a real robotic manipulator. Before being able to perform the experiment some implementation issues had to be solved. In order to build an observer for the robot, a system identification for the robot Joint 1 and for the gravity torques $G(q)$ was done. The resolvers used to measure the joint positions introduced a nonlinearity that had to be compensated.

## 6.2 Gravity Compensation

We assume the following simplified model for Joints 2 and 3 of the industrial robot ABB irb 2000 in Figure 6.1. The equations of the gravity torques in Joints 2 and 3 assuming a simple friction model $f = c \cdot sign(\dot{q})$ can be written

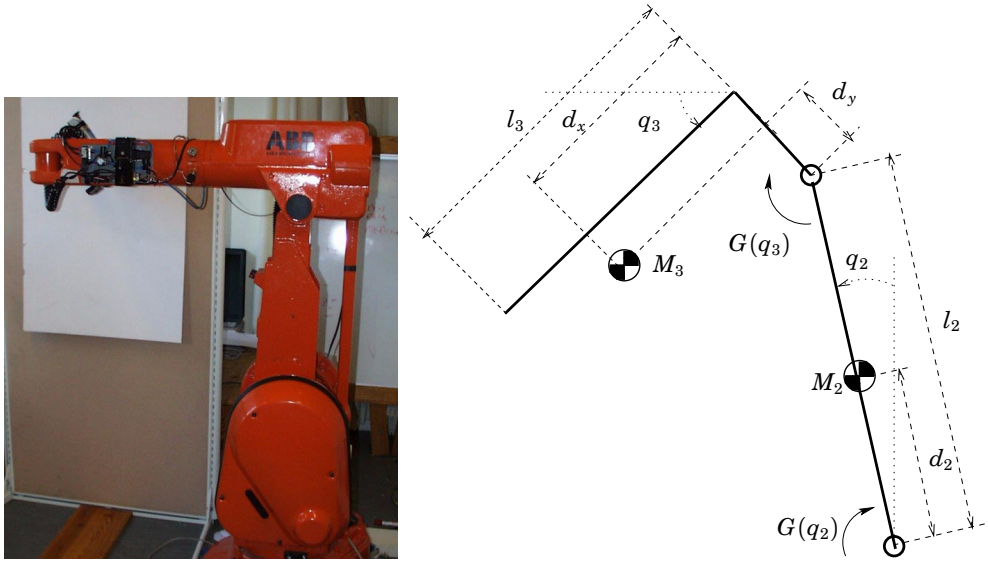


**Figure 6.1** Robot manipulator scheme for gravity compensation.

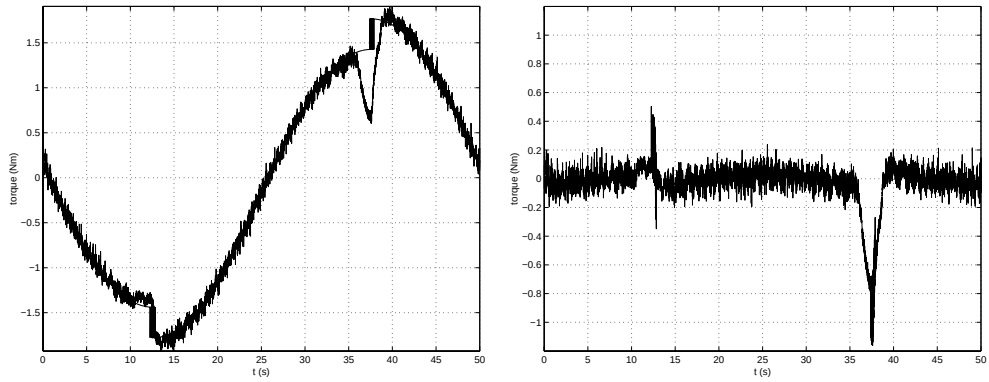


**Figure 6.2** Estimation of the gravity torque in Joint 2. Left: Measured torque and estimated. Right: Torque estimation error.

$$\begin{aligned} G(q_3) &= M_3 g \left[ d_x \cos\theta_3 + d_y \sin\theta_3 \right] + c_3 \ \text{sign}\{\dot{\theta}_3\} \\ &= \lambda_1 \cos\theta_3 + \lambda_2 \sin\theta_3 + \lambda_3 \ \text{sign}\{\dot{\theta}_3\} \end{aligned} \tag{6.1}$$

$$\begin{aligned} G(q_2) &= M_3 g \left[ d_x \cos\theta_3 + d_y \sin\theta_3 + l_2 \sin\theta_2 \right] + M_2 g d_2 \sin\theta_2 \\ &\quad + c_2 \ \text{sign}\{\dot{\theta}_2\} \\ &= \lambda_4 \left[ \lambda_1 \cos\theta_3 + \lambda_2 \sin\theta_3 \right] + \lambda_5 \sin\theta_2 + \lambda_6 \ \text{sign}\{\dot{\theta}_2\} \end{aligned} \tag{6.2}$$

where

$$\begin{aligned} \lambda_1 &= M_3 g d_x \\ \lambda_2 &= M_3 g d_y \\ \lambda_3 &= \text{Friction coefficient of Joint 3} \\ \lambda_4 &= \text{Relation between motor torques 2 and 3} \\ \lambda_5 &= M_3 g l_2 + M_2 g d_2 \\ \lambda_6 &= \text{Friction coefficient of Joint 2} \end{aligned}$$

Using least squares identification [17] it is possible to identify all the parameters $\lambda_i$. As $\Gamma_{g3}$ only depends on $\theta_3$, we first determined $\lambda_1$,$\lambda_2$ and $\lambda_3$. Then, using $\lambda_1$ and $\lambda_2$ the remaining parameters were obtained:

$$\begin{aligned} &\lambda_1 = 1.5545 && \lambda_2 = 0.4610 && \lambda_3 = -0.1764 \\ &\lambda_4 = -0.0045 && \lambda_5 = -3.0194 && \lambda_6 = 0.1696 \end{aligned}$$

The results of the gravity torques estimation is shown in Figures 6.2 and 6.3. In the experiment, a position trajectory reference was given and the resulting control torques were recorded. The controller was active and, as we will study later, the resolver nonlinearity introduced in the closed loop a high disturbance which effects can be easily seen in the torque signals. The position reference trajectory was an ellipsoid, similar to the final experimental setup, to cover a wide part of the manipulator workspace. The velocities were kept very low in order to minimize inertia effects. However, in fig 6.2 between $t = 35-40\ s$ we can see an important error caused by the influence of inertia torques in a special configuration of the manipulator during the experiment. Another thing that can be noticed from the results

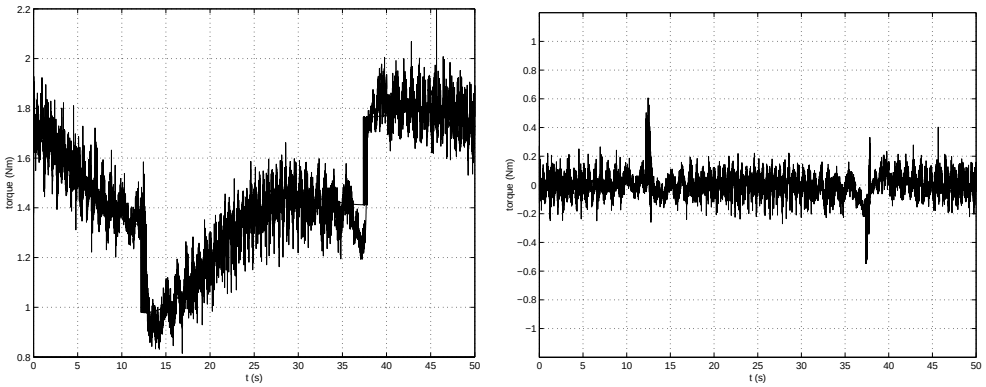


**Figure 6.3** Estimation of the gravity torque in Joint 3 and its estimation error.

is the low accuracy of the model when the velocity is close to zero ($t \approx 12s$ and $t \approx 37s$). This is due to the simplified friction model used, which is not very realistic for velocities close to zero.

## 6.3 Resolver Nonlinearity Compensation

The resolvers used to measure the joint angles introduce a slight nonlinearity almost imperceptible. The problem arises when the position measurements are differentiated to obtain velocity estimates. Then, the influence of this nonlinearity becomes more important and it makes it necessary to compensate for. We can see a scheme of the problem in Figure 6.4. The diagonal dotted line is the ideal position measurement and the solid line is the real measured position.

As a first approach we tried to model the nonlinearity as a sum of sinusoidals. That is

$$q_m = q + \sum_k a_k \sin(kq + \phi_k) \tag{6.3}$$

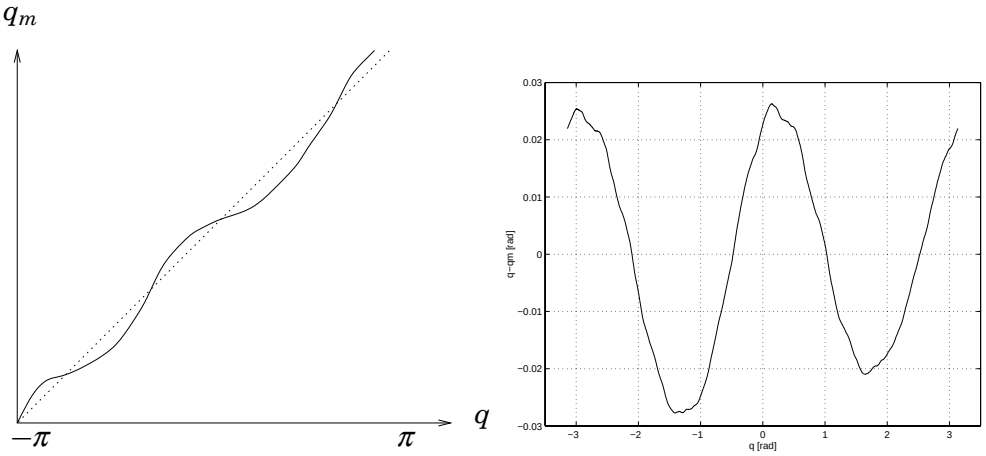


**Figure 6.4** Left:Resolver nonlinearity problem. Real position $q$ and measured position $q_m$. Right: Estimated shape of the resolver nonlinearity.

which can be approximated by

$$q_m \approx q + \sum_k a_k \sin(kq_m + \phi_k) \tag{6.4}$$

$$= q + \sum_k \alpha_k \sin(kq_m) + \beta_k \cos(kq_m) \tag{6.5}$$

with

$$\alpha_k = a_k \cos(\phi_k) \tag{6.6}$$

$$\beta_i = a_k \sin(\phi_k); \tag{6.7}$$

Equation (6.5) is linear in parameters so a standard Least Squares problem can be formulated. The main problem is to obtain a consistent data of the nonlinearity $q_m - q$. One way of obtaining an ideal estimate of $q - q_m$ would be to keep the velocity at a constant value and simply De-trend the resulting position measurements. This is not easy for different reasons. When doing identification experiments the controller had to be turned off. Otherwise the effect of the nonlinearity gets inside the feedback loop destroying the validity of the data. It was found that the main modes of the nonlinearity were $k = 2$ and $k = 1$. The Least Squares problem was solved and the resulting parameters were

$$\begin{aligned} a_2 &= 0.0324 & \phi_2 &= 0.8421 \\ a_1 &= 0.0027 & \phi_1 &= -1.0316 \end{aligned} \tag{6.8}$$

It seems that there is also a small amplitude high frequency term ($k \approx 14$) that was very hard to identify. The results of the compensation are shown in Figure 6.5.

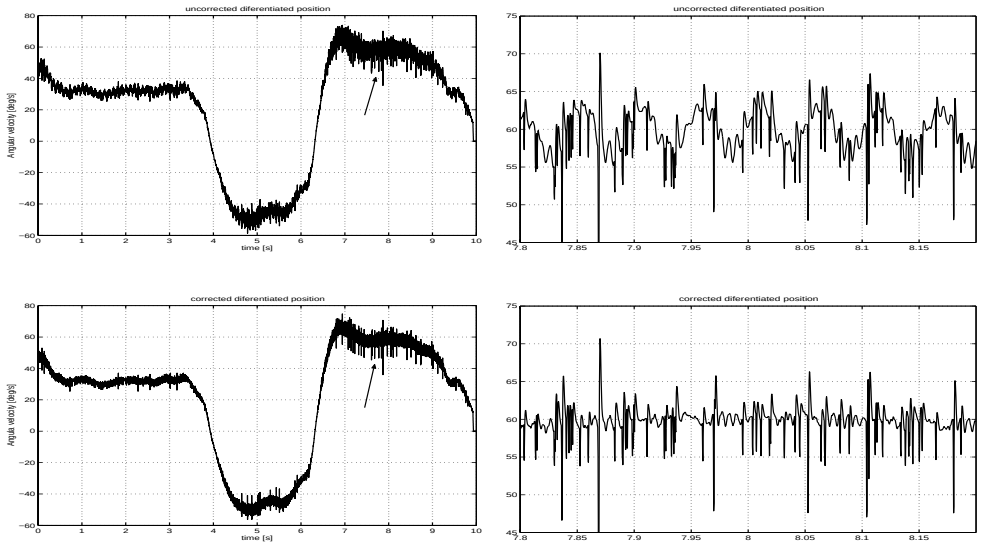


**Figure 6.5** Uncorrected and corrected velocity estimates. We see how quantitatively the improvement is not big, but notice that the main component of the nonlinearity which causes the oscillation has been eliminated. There is still a very characteristic kind of peaks that we will try to eliminate.

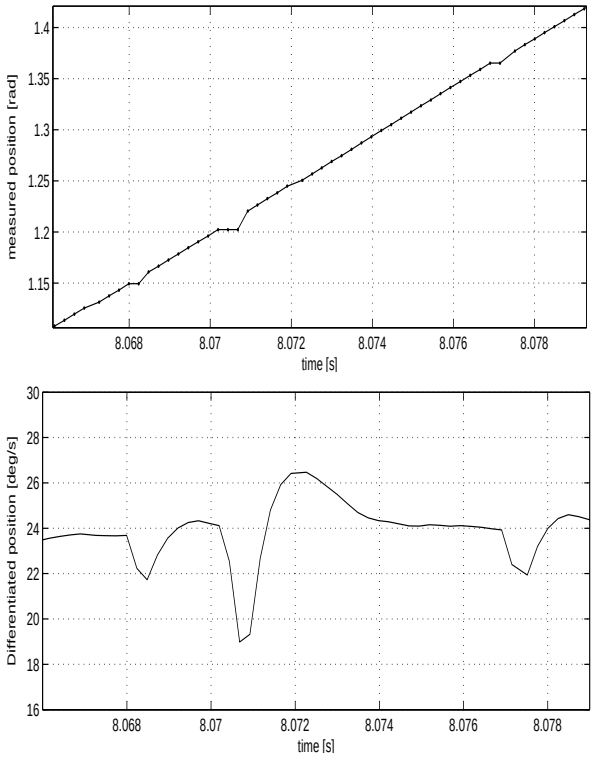


**Figure 6.6** Position measurement signal with sequences of two and three consecutive identical samples. The position signal is differentiated and low-pass filtered to produce velocity estimates in which the effect of the identical samples can be easily seen.

At a first sight, it seems that the compensation does not improve substantially the velocity estimates. If we have a closer look we see that the fundamental mode of the nonlinearity has been eliminated while there is a lot of pronounced peaks that are still remaining. It was found that this peaks had nothing to do with the resolver nonlinearity but with a strange feature of the measured position signal. We studied the raw unfiltered position signal coming from the robot system and found that these peaks are produced by sequences of consecutive identical samples (Figure 6.6). The number of consecutive equal samples of these sequences is typically two or three. Although in some exceptional cases we founded up to four equal samples. The reason for this problem has not been found yet at the moment of this thesis, and is probably a communication problem between the robot sensors and the data acquisition system. As we needed to solve this problem as fast as possible we implemented an alternative provisional solution. A causal nonlinear filter was designed to reconstruct these identical samples using information only from the past samples. It was conceived to reconstruct up to three consecutive samples and it didn't introduce any sample delay in the system. The results of the compensation including the nonlinear filter is shown in Figure 6.7. The fundamental mode of the nonlinearity and the peaks have been eliminated.

Note that the resolver nonlinearity would be a good reason to use an observer and to avoid *dirty derivatives*.

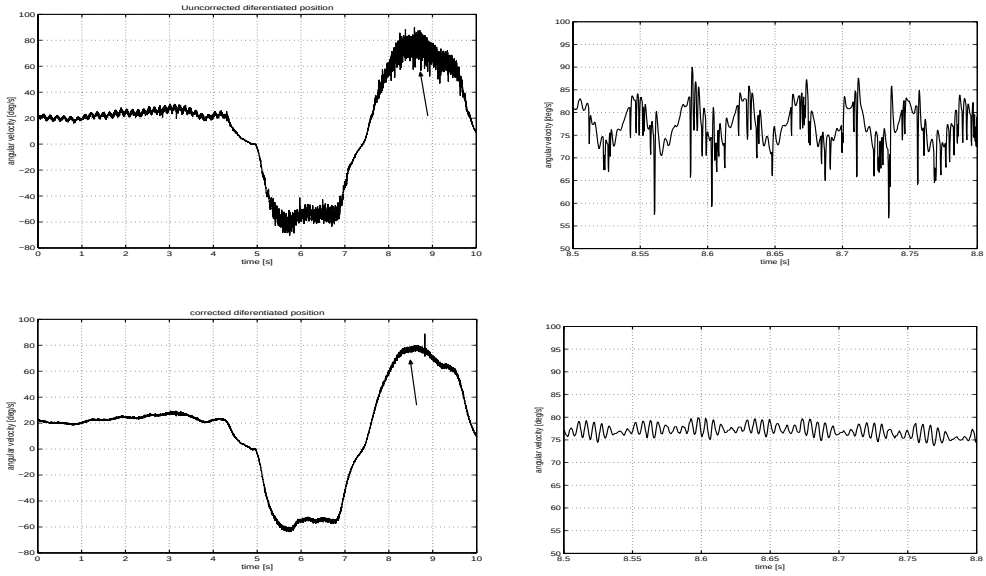


**Figure 6.7** Uncorrected and corrected velocity estimates after the noise filtering. The main mode of the nonlinearity and the characteristic signal noise have been eliminated. Notice (down left, $t \approx 9s$) the existence of a peak in the compensated velocity signal. The nonlinear filter was implemented to compensate when finding up to three consecutive equal samples. In this case there were four consecutive equal samples.

## 6.4 System Identification of Joint 1

In order to build an observer for the robot manipulator we need to obtain a suitable model and identify the corresponding parameters. We considered the following model structure for robot Joint 1

$$m_{11}\ddot{q}_1 + d_1 \text{sign}\{\dot{q}_1\} + d_2\dot{q}_1 + b = \tau_1 \tag{6.9}$$

$$m_{11} = a_1 + a_2 \sin^2 q_2 + a_3 \sin q_2 \tag{6.10}$$

where $m_{11}$ represent the inertia of Joint 1 depending only on $q_2$. This holds since in the experiments only Joints 1 and 2 will move so that $q_3 = 0$. The torque offset $b$ turned out to be important, despite it has not been considered before.

An open-loop identification experiment was performed using the *PRBS* signal of Figure 6.8 as a torque reference for Joint 1 and an ellipsoidal position reference for Joint 2. A Least Squares problem was formulated to identify the continuous time model (see [17, p.255]). We used "state-variable filters" $F_0, F_1$ acting on the inputs and outputs of the system

$$F_0 = \frac{1}{s+1}, \qquad F_1 = \frac{s}{s+1} \tag{6.11}$$

and obtained the following filtered signals:

$$q_{1f} = F_0 q_1, \quad q_{2f} = F_0 q_2, \quad \dot{q}_{1f} = F_0 \dot{q}_1$$
$$\ddot{q}_{1f} = F_1 \dot{q}_1, \quad \tau_{1f} = F_0 \tau_1$$

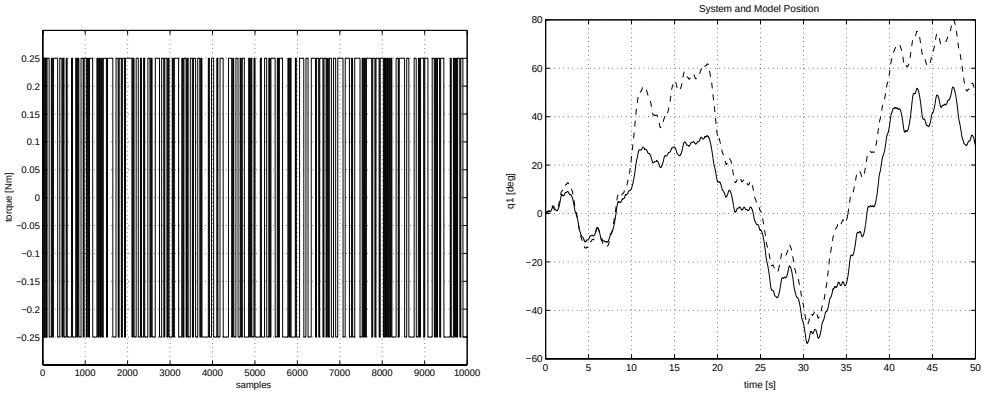


**Figure 6.8** Left:*PRBS* signal used in the identification experiments. Right: Outputs from the Robot and from the estimated model

The LS problem becomes

$$\tau_{1f} = \Phi\theta + e \tag{6.12}$$

with regressor matrix $\Phi$ and vector of unknown parameters $\theta$

$$\Phi = [\,\ddot{q}_{1f} \quad \ddot{q}_{1f}\sin^2 q_{2f} \quad \ddot{q}_{1f}\sin q_{2f} \quad \text{sign}\{\dot{q}_{1f}\} \quad \dot{q}_{1f} \quad 1\,] \tag{6.13}$$

$$\theta = [\,a_1 \quad a_2 \quad a_3 \quad d_1 \quad d_2 \quad b\,]^T \tag{6.14}$$

The parameters obtained were

$$a_1 = 0.0025 \qquad a_2 = 8.9392 \cdot 10^{-5} \qquad a_3 = 8.1131 \cdot 10^{-5} \tag{6.15}$$

$$d_1 = 0.0385 \qquad d_2 = 0.0047 \qquad b = -0.0015 \tag{6.16}$$

The Robot position and the position of the obtained model during the experiment are shown in Figure 6.8.

## 6.5 Force Observer

First we will write (6.9) in state space form as

$$\begin{cases} \dot{x}_2 = [\tau_1 + \Gamma_F - d_1\text{sign}\{x_2\} - d_2 x_2 - b]\dfrac{1}{m_{11}} \\ \dot{x}_1 = x_2 \\ m_{11} = a_1 + a_2\sin^2 q_2 + a_3\sin q_2 \end{cases} \tag{6.17}$$

where $x_1 = q_1$, $x_2 = \dot{q}_1$ and $\Gamma_F$ is the disturbance torque produced by the environmental force $F$. Then we construct an observer as

$$\begin{cases} \dot{\hat{x}}_2 = [\tau_1 - d_1\text{sign}\{\hat{x}_2\} - d_2\hat{x}_2 - b]\dfrac{1}{m_{11}} + K_2\tilde{x}_1 \\ \dot{\hat{x}}_1 = \hat{x}_2 + K_1\tilde{x}_1 \\ \tilde{x}_1 = x_1 - \hat{x}_1 \\ m_{11} = a_1 + a_2\sin^2 q_2 + a_3\sin q_2 \end{cases} \tag{6.18}$$

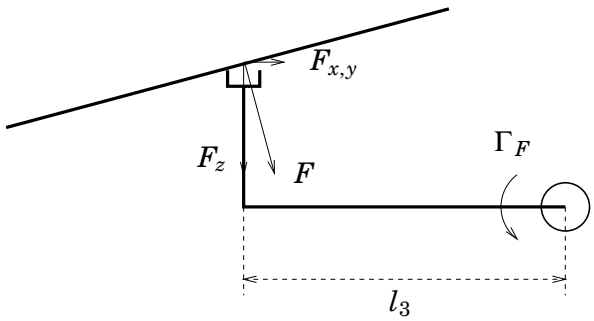


**Figure 6.9** The contact force $F$, normal to the surface, generates a disturbance torque $\Gamma_F$. The force sensor gives measurements of $F_z$ and $F_{x,y}$.

and following the same methodology we used in the previous chapters, the observer estimation error dynamics yields

$$m_{11}\ddot{\tilde{x}}_1 + (d_2 + m_{11}K_1)\dot{\tilde{x}}_1 + (d_2K_1 + m_{11}K_2)\tilde{x}_1 = \Gamma_F \tag{6.19}$$

and the environmental torque can be estimated by

$$\hat{\Gamma}_F = (d_2K_1 + m_{11}K_2)\tilde{x}_1 \tag{6.20}$$

The observer gains $K_1$ and $K_2$ are chosen such that the estimator has two equal real poles. This holds when

$$K_2 = \frac{(a_1K_1 - d_2)^2}{4a_1^2} \tag{6.21}$$

Around $q_2 = 0$ we can approximate $m_{11} \approx a_1$. Notice that with this force observer what we really estimate is the environmental torque $\Gamma_F$ and making use of the robot geometry is possible to estimate the contact force in the gripper direction $F_z$ as

$$\hat{F}_z = \frac{1}{l_3}\hat{\Gamma}_F \tag{6.22}$$

In order to compare the measurements of the force sensor and the estimated forces we will use the measurement $F_z$ perpendicular to the robot gripper coming from the sensor. This is a good approximation as long as the contact force is perpendicular to the gripper and can be assumed equal to $F_z$.

## 6.6 Experiment I

In the first experiment the robot manipulator was situated in front of a blackboard and a square torque reference was given for Joint 1. A scheme of the experimental setup can be seen in Figures 6.10-6.9. We tried to place the blackboard so that it was perpendicular to the robot gripper when having contact. In practice, the real contact force $F$ was not exactly perpendicular so it also generated forces $F_{x,y}$ in the force sensor.

The results of Experiment 1 are shown in Figure 6.11.

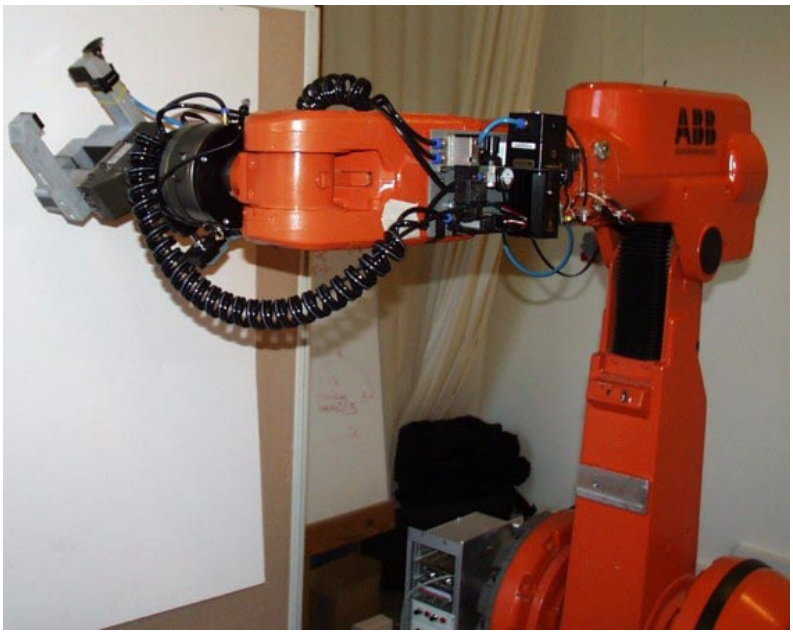

**Figure 6.10** Experimental setup.

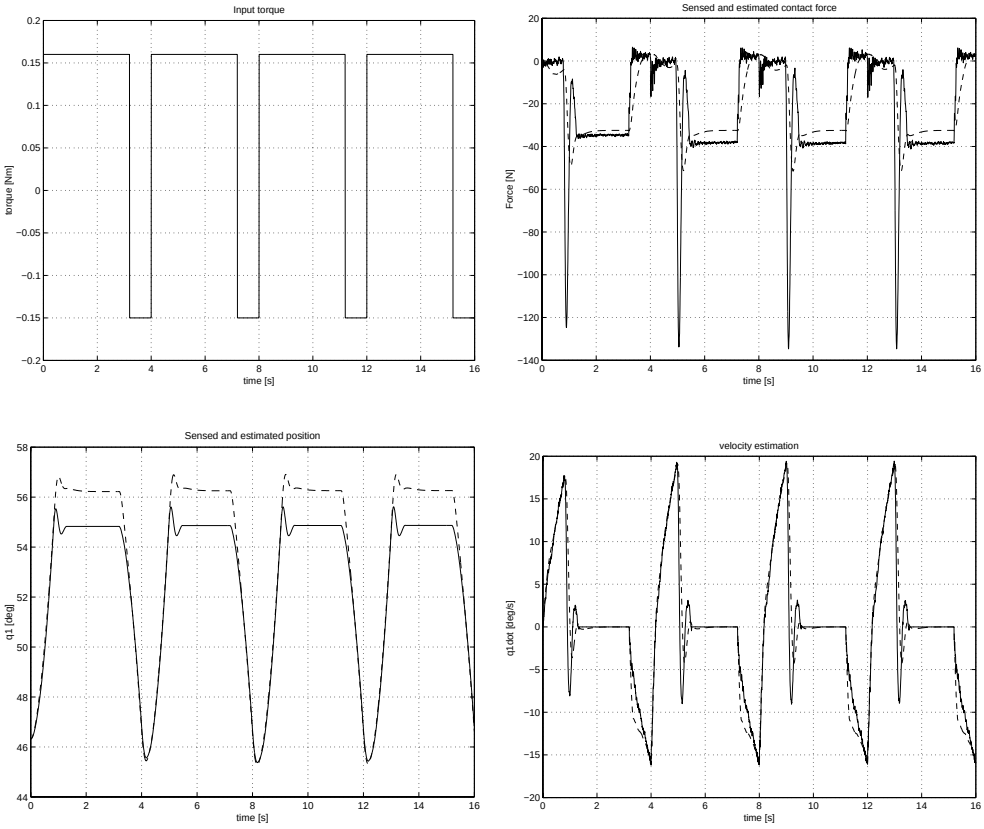


**Figure 6.11** Results of Experiment I. Right-Up the force sensor signal (solid line) and the estimated environmental force (dashed). The estimated position (dashed), Left-Down, follows the sensed position (solid) in free movement, but when in contact there is a structured error that makes possible the force estimation.

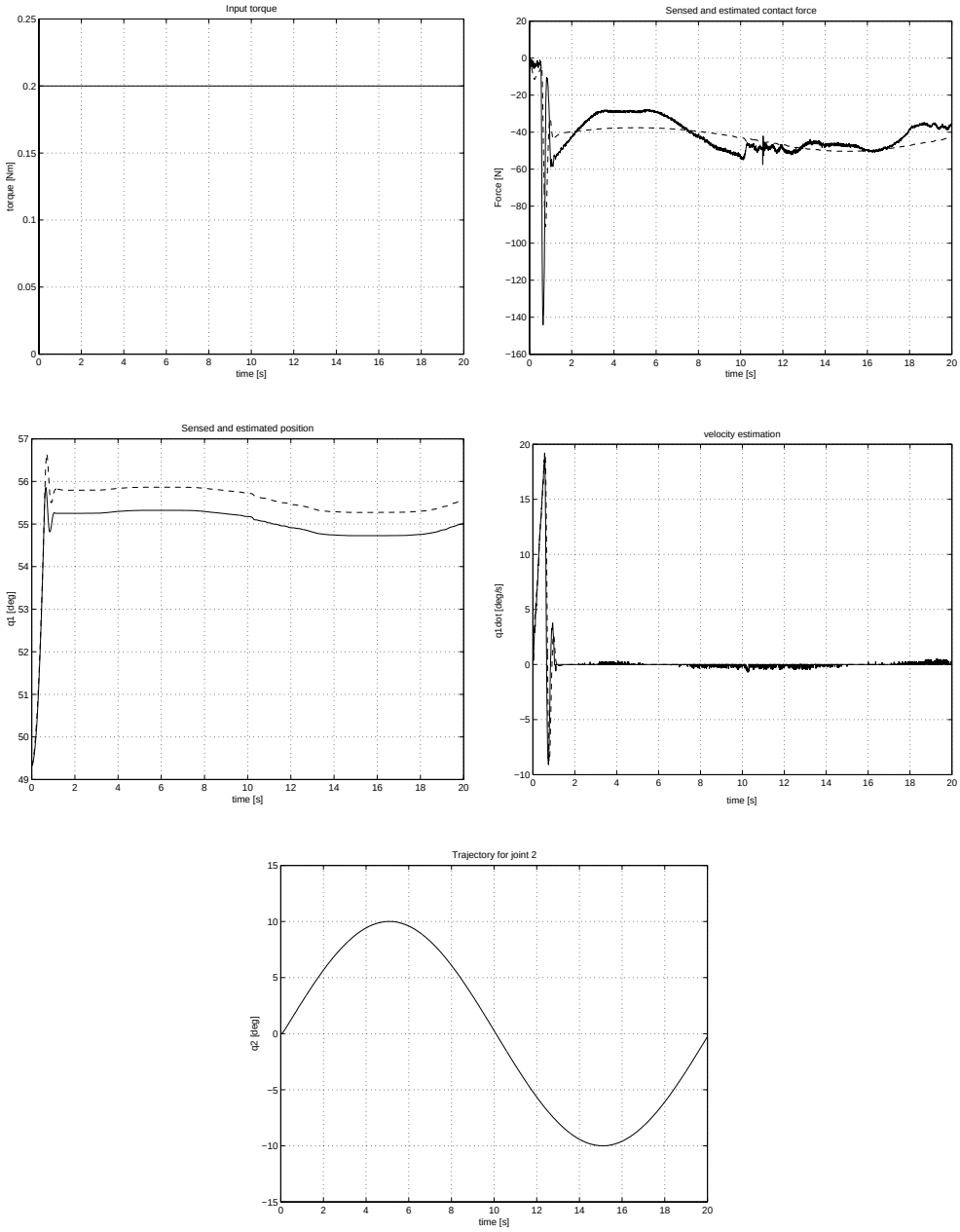


**Figure 6.12** Results of Experiment II. Force estimation while the robot manipulator is moving in a circle in contact with the blackboard. The inertia $m_{11}$ changes with Joint 2 and the same constant torque produces different contact forces.

## 6.7 Experiment II

In the second experiment the robot moved as drawing a circle in the blackboard. A constant reference torque was given for Joint 1 and an ellipsoidal position reference was given for Joint 2. The forces $F_{x,y}$ non perpendicular to the gripper were much bigger during this experiment due to the friction between the blackboard and the gripper.

The results from Experiment 2 are shown in Figure 6.12.

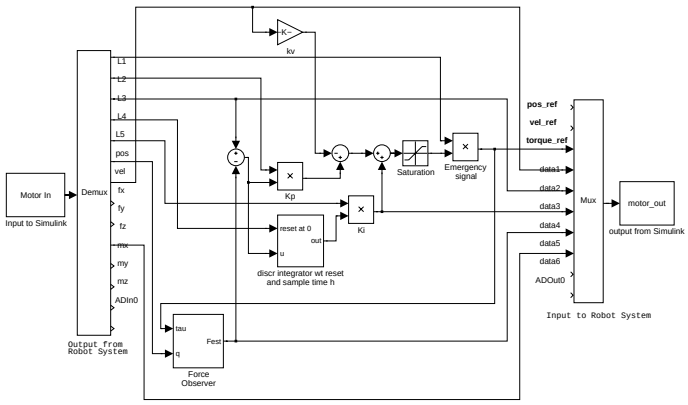


**Figure 6.13** Simulink model used in the experiments.

## 6.8 Force Control using the Force Observer

In this section it would be shown how the Force Observer can be used succesfully to perform a common force control task. The main objective is to use the Force Observer to control the contact force between the robot end-effector and the blackboard.

The ABB control computer hardware has been replaced by an external VME-based control computer. The servo motors on the joints, the resolvers, the power supply electronics and the safety board remains from the original system. Matlab/Simulink and the Real-Time Workshop (RTW) have been used for the industrial robot force control implementation. This toolbox produces code directly from Simulink models and automatically builds programs that can be run in a variety of environments. Figure 6.13 shows the Real-Time Workshop scheme used for the IRB2000 force control. The blocks Input to Simulink and Output from Simulink are S-Function written in C that communicates the external modules with the Simulink inputs and outputs. In this case we have 5 parameters inputs (L1..L5), the position and the velocity of the IRB-2000 and the robot forces and torques. The parameter inputs can be varied using a graphical parameter user interface developed in the Department. It is a front-end interface on the workstation, which allows the user to adjust the parameters of the controllers during run-time. In this case we use the L1 parameter input as emergency signal, L2 as the $K_p$ gain, L3 as force input reference, L4 as reset signal for the integral action, and L5 as the $K_i$ gain.

The implemented force controller consists of a proportional and integral part on the force error and a derivative term on the robot velocity.

$$\tau_c = K_p(F_{ref} - \hat{F}) + K_i \int (F_{ref} - \hat{F})\mathrm{d}t - K_v \dot{q} \tag{6.23}$$

In the experiment a reference contact force was given varying from 0 to $60N$. Experimental results can be seen in figures 6.14 and 6.15.

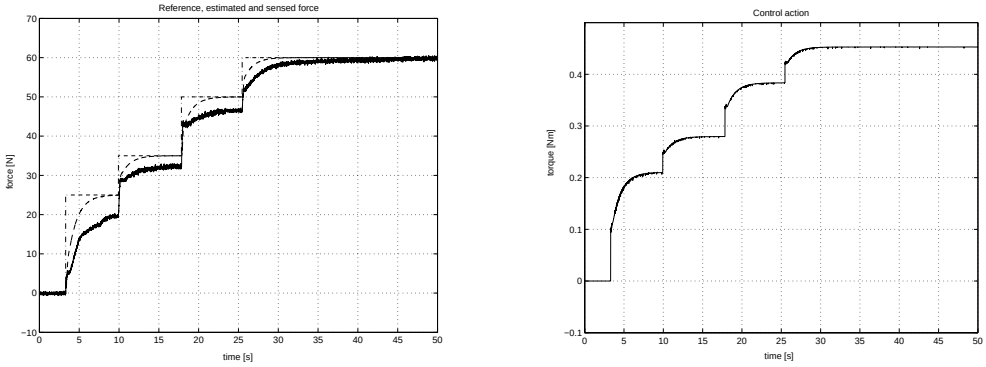


**Figure 6.14** Left graph Reference force $F_{ref}$ (dash-dot), sensed contact force $F$ (solid) and estimated contact force $\hat{F}$ (dashed). Right graph input control sognal $\tau_c$

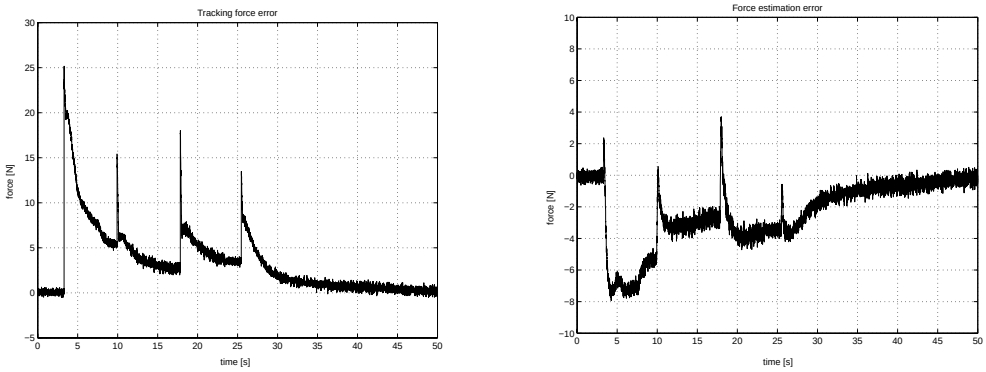


**Figure 6.15** Left graph sensed force tracking error $F_{ref} - F$. Right graph force estimation error $F - \hat{F}$.

## 6.9 Discussion

The final implementation of the resolver compensation in the robot system implied the construction of a look-up table with the values of the modeled nonlinearity. This increased the computational efficiency of the compensation. By using the look-up table the need for explicit identification of the amplitude and phase of the harmonics could be by-passed. We directly construct the table with the estimated values of the nonlinearity. Various experiments were done until obtaining an estimate of the shape of the nonlinearity (Figure 6.4).

The experiments show the good behavior of the Force Observer even with the use of a very simplified model of the robot manipulator. The output injection in the observer seem to be extremely efficient in compensating possible parameter and structural model errors, while the environmental forces were still able to deflect over them and produce consistent position estimation errors.

### Friction Considerations

When applying the Force Observer to systems with friction some important considerations need to be done. Assume the simplified friction model with stiction shown in figure 6.16 where the friction force is plotted as a function

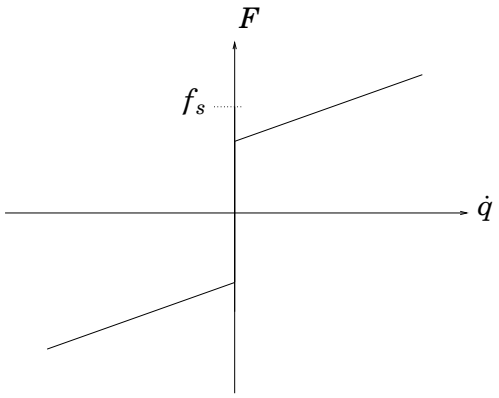


**Figure 6.16** Friction model considering stiction, viscous and Coulomb components.

of the velocity. If the system has zero velocity, all the environmental forces smaller that the value $f_s$ will not produce any effect on the system dynamics either on the Force Observer. This means that the Force Observer is *blind* to the scale of forces smaller than the stiction threshold $f_l$.

# 7. Concluding Remarks

## 7.1 Conclusion

A model based Force Observer for Vehicles and Robot Manipulators has been introduced. Several simulations and an experiment with an Industrial Robot have proven the versatility of this sensor-less approach to force estimation. It has also been shown how the Force Observer for robotic manipulators can be successfully integrated in a common force control architecture.

The performance of the Force Observer depends mainly on how good models we can obtain. This is actually a theoretical limitation which can be trespassed with a meticulous system identification procedure. In the Robot experiments we saw how our simplified model behaved reasonably well, in part due to the stabilizing effect of the output injection. However, we should notice that using the introduced Force Observer all the estimation errors are directly attributed to environmental forces, which can lead to important force estimation errors when dealing with poor models.

Noise sensitivity of the Force Observer has also been pointed out as a major source of possible errors. This is specially clear in the linear case, where we showed the high pass characteristic of the force estimation error transfer function.

The observer gains play an extremely important role in the force estimation performance. It has been shown how the $\Lambda$ matrices are coefficients of an imaginary damped spring mass system, and how the observer gains can be used to shape these coefficients. Different approaches to the choice of these gains and how they must balance the trade between sensor quality, noise characteristics and estimation performance has also been presented.

## 7.2 Future Work

In the mark of this master's thesis there is still theoretical and practical work that can be done. One important implementational aspect to be solved is the formulation of a systematic procedure for the choice of the observer gains. As it was mentioned before, an optimization problem could be solved in which some information about the environmental forces and the system noises is assumed to be known.

An environmental Force Observer in ship dynamics has also been introduced. One possible extension would be to integrate this estimation in the passive nonlinear observer introduced by T. I. Fossen and J. P. Strand in [7].

All the robot experiments have been done with a simplified model of Joint 1. It would be very interesting to obtain a more complex model of the robot with more degrees of freedom and use it to design more interesting force control experiments.

# 8. Bibliography


[1] P. J. Hacksel and S. E. Salcudean, "Estimation of Environmental Forces and Rigid-Body Velocities using Observers." Proc. of 1994 IEEE Int. Conf. on Robotics and Automation, pp. 931-936, 1994.

[2] S. Nicosia and P. Tomei, "Robot control by using only joint position measurements", IEEE Transactions on Automatic Control, Vol. 35, No. 9, pp. 1058-1061, September 1990.

[3] K. Ohishi, M. Miyazaki, M. Fujita and Y. Ogino, "$H^{\infty}$ Observer Based Force Control without Force Sensor", Proceedings of IEEE Int. Con. on Industrial Electronics, Control and Instrumentation, pp. 1049-1054, 1991.

[4] A. Robertsson, *On Observer-Based Control of Nonlinear Systems*, PhD thesis, Dept. Automatic Control, Lund Institute of Technology, 1999.

[5] T. I. Fossen, *Guidance and Control of Ocean Vehicles*. New York: Wiley, 1994.

[6] T. I. Fossen and Å. Grøvlen, "Nonlinear Output Feedback Control of Dinamically Positioned Ships using Vectorial Observer Backstepping." IEEE Transactions on Control Systems Technology, Vol. 6, No. 1, pp. 121-128, January 1998.

[7] T. I. Fossen and J. P. Strand, "Passive Nonlinear Observer Design for Ships using Lyapunov Methods: Full-Scale Experiments With a Supply Vessel." *Automatica*, 35:1, pp. 3-16, 1999.

[8] T. I. Fossen, "Nonlinear Passive Control and Observer Design for Ships" Tutorial Workshop, ECC'99, Karlsruhe, Germany, August 1999.

[9] A. Robertsson and R. Johansson, "Comments on Nonlinear Output Feedback Control of Dinamically Positioned Ships using Vectorial Observer Backstepping". IEEE Transactions on Control Systems Technology, 1998.

[10] F. Calugi, A. Robertsson and R. Johansson, "An Adaptive Observer for Control of Dynamically Positioned Ships using Vectorial Observer Backstepping". CDC02-REG0522.

[11] F. Calugi, "Observer-based Adaptive Control", Master's thesis, Dept. Automatic Control, Lund Institute of Technology, April 2002.

[12] D. Henriksson, "Observer-based Impedance Control in Robotics", Master's thesis, Dept. Automatic Control, Lund Institute of Technology, November 2000.

[13] B. Siciliano and L. Villani, *Robot Force Control*, Kluwer academic publishers, 1999.

[14] D. M. Gorinevsky, A. M. Formalsky and A. Y. Schneider, *Force Control of Robotic Systems*, CRC Press, 1997.

[15] R.M. Murray, Z. Li and S.S. Sastry, *A Mathematical Introduction to Robotic Manipulation*, CRC Press, 1994.

[16] W. Khalil and E. Dombre, *Modeling, Identification and Control of Robots*, Hermes Penton Science, 2002.

[17] R. Johansson, *System Modeling and Identification*, Prentice Hall, 1993.

[18] B.D.O. Anderson and J.B. Moore, *Optimal Control*, Prentice-Hall International, 1989.

[19] B.D.O. Anderson and J.B. Moore, *Optimal Filtering*, Prentice-Hall, 1979.

[20] N. Wiener, *Extrapolation, Interpolation and Smoothing of Stationary Time Series*, Cambridge, Mass: M.I.T. Press, 1949.

[21] J.S.Meditch, *Stochastic Optimal Linear Estimation and Control*, McGraw-Hill, 1969.

[22] H. Khalil, *Nonlinear Systems*, second edition, Prentice-Hall, 1996.

[23] J-J.E. Slotine and W. Li, *Applied Nonlinear Control*, Prentice Hall, 1991.

[24] R. Ortega, A. Lorìa, P.J. Nicklasson and H. Sira-Ramirez, *Passivity-based Control of Euler-Lagrange Systems*, Springer, 1998.

[25] K.J. Åstrom and B. Wittenmark, *Computer Controlled Systems*, Prentice-Hall, 1984.

[26] W.J. Rugh, *Linear System Theory*, Prentice-Hall, 1993.

# A. Matlab Code

## A.1 Resolver Nonlinearity Identification

```
%----  IDENTIFICATION OF THE RESOLVER NONLINEARITY ----
global in
global inp_X resp_X;
%--- Defining input signals for the experiments-----
% square signal >>> Torque references
clear in
T1=1.4;
T2=15;
tsamp=0.005;
iend1=T1/tsamp;
iend2=T2/tsamp+iend1;
in(1:iend1)=0.17;
in(iend1:iend2)=0.12;
%square with initial ramp  >>> Velocity references
A=20;
Tramp=1;
Tend=15;
tsamp=0.005;
iramp=Tramp/tsamp;
iend=Tend/tsamp
i(1)=0;
for i=2:(iramp)
  in(i)=A*(i)/(iramp);
end
for i=iramp:iend
  in(i)=A;
end

%--- Sending data to Exc_handler
Exc_handler('update_input',1,in,'replace');
% 13 == velocity ref Joint 1 (remember to set Kpos=0)
% 1  == torque reference Joint 1 (remember to set RegOff(1))
% 7  == position reference Joint 1
%----  Using slaveplot the experiments have been recorded
%----  Ideally a sequence of constant velocity is obtained
%----  SSdata == [t q u usat qdot [] [] rawq  ... ]
t=SSdata(:,1);
t=t-t(1);
qm=SSdata(:,2);    % filtered and linked position
qmdot=SSdata(:,5); % diferentiated and filtered position
rqm=SSdata(:,8);   % unfiltered unlinked raw position
%----  qm    == Position filtered
%----  qmdot == Position diferentiated and filtered position
%----  rqm   == Raw position unfiltered unlinked >> rqm in [-pi,pi]
%----           within one motor turn

clear tc;                    % determining blocks
tc(1)=1;                     % within one motor turn
p=2;                         % tc == vector of block index
for i=1:length(rqm)-1
  if abs(rqm(i)-rqm(i+1))>1
    tc(p)=i;
```

```
    p=p+1;
  end
end

%---- Defining identification data and visualization.
%---- Blocks within one motor turn are assumed with constant
%---- velocity. Then the blocks are de-trended and the nonlinearity
%---- phenomena becomes plausible. A mapping between time and angle
%---- can be done under constant velocity assumption.

figure
hold off
R=[];
Rtable=[]; % data for the construction of the look-up table
tR=[];
res=(2*pi)/(2^14);
angle_scale=[-pi:10*res:pi];
for i=1:length(tc)            % we can choose the identification sequence
  z=rqm(tc(i-1)+1:tc(i));     % creating a block
  z=med_filter_resolver(z);   % peack reduction filter
  tz=-pi+(0:(2*pi)/length(z):2*pi-(2*pi)/length(z))';   % block angle scale
  z=z-((z(length(z))-z(1))/(tz(length(tz))-tz(1)))*tz;  % de-trending
  z=detrend(z,'constant');
  R=[R;z];           % vector of blocks
  tR=[tR;tz];        % vector of angles
    %------
     tmp=[];
     for angle=angle_scale
       tmp=[tmp interp1(tz,z,angle)];
     end;
     Rtable=[Rtable; tmp];
    %-----
  plot(tz,z)
  hold on
  grid on
  pause                       % visualization
end

%-----------  SINUSOIDAL IDENTIFICATION    -----------------------

%----  Least Squares formulation
%----  yfit=a2*sin(2*q+fi2) + a1*sin(q+fi1)
%----  yfit=[a2*cos(fi2)]*sin(2q)+[a2*sin(fi2)]cos(2q)=REG*theta

REG=[sin(2*tR) cos(2*tR) sin(tR) cos(tR)];

theta=inv(REG'*REG)*REG'*R;
a2=sqrt(theta(1:2)'*theta(1:2));         % a2      =0.0324
fi2=atan(theta(1)/theta(2));             % fi2     =0.8421
a1=sqrt(theta(3:4)'*theta(3:4));         % a1      =0.0027
fi1=atan(theta(3)/theta(4));             % fi1     =-1.0316

%-----------  LOOK-UP TABLE APPROACH    -----------------------
%%---- Defining shape of nonlinearity for look-up table

global nl nllong bias
nl=mean(RRR);
bias=nl(1);   % we separate the nonlinearity by nl (nl(1)==0)
nl=nl-bias;   % and bias, (bias==nl(1))
nllong=interp(nl,10); % resample

%---------- VALIDATION ----------------------------------------
```

```
%---- validation data loaded, SSdata_validation >> qm, rqm, qmdot...

%---- Non corrected position rqm motor
xl=fast_link_resolver(rqm); % links the raw position
xl=med_filter_resolver(xl); % nonlinear filter, peack filtering
%---- Corrected look-up table rqm motor
rqmcorr=correct_resolver_table(rqm);
qmcorr=fast_link_resolver(rqmcorr);
qmcorr=qmcorr+bias;
qmcorr=med_filter_resolver(qmcorr);
%---- Corrected sinusoidals rqm motor
rqmcorr=rqm-a2*sin(2*rqm+fi2)-a1*sin(rqm+fi1);
qmcorr=link_resolver(rqmcorr);
qmcorr=med_filter_resolver(qmcorr);
%---- Perform filtering and derivating from 'robot_filters.mdl'
%---- UnfilteredPosition  -> FilteredPosition, FilteredVelocity
%---- UnfilteredPosition = [time' qmcorr']
time=(0:1/4e3:(length(qmcorr)-1)/4e3)';
UnfilteredPosition = [time qmcorr];

sim('robot_filters');  % simulink model
```

## A.2 Look-up Table for Nonlinearity Compensation

```
%---    Table For Resolver compensation
%---    Stored in 'resolver1comp_alex.txt'
%---   and 'resolver1bias_alex.txt'
%---
%---    0,0,0,0,0,0,0,0,
%---   0,0,0,0,0,0,0,0,
%---    ..............
%---   0,0,0,0,0,0,0,0,
%---    2^12 rows;  2^14=16384 integer values of the nonlinearity
%---    scaled by [0:2*pi]->[0:16383]

% compensation parameters %
% vector nllong=interp(nl,10), length(nllong)=16390
% bias, bias=0.0219 global variables nllong and bias

global nllong bias

fid= fopen('resolver1comp_alex.txt','w');
fidbias=fopen('resolver1bias_alex.txt','w');

fprintf(fidbias,'%d \n',-bias);

p=1;
for i=1:16383
  z=round(-nllong(i)*(32768/(pi)));
  if p~=8
    fprintf(fid,' %d , ',z);
    p=p+1;
  elseif p==8
    fprintf(fid,' %d , \n ',z);
    p=1;
  end
end
```

```
z=(-nllong(16384)/16384)*2*pi;
z=round(z);
fprintf(fid,' %d \n ',z);
```

## A.3 Peak Filtering ( .mod file)

```
IF i=0 THEN
   vPos[3] :=vPos[2];           (* Update of vPos  *)
   vPos[2] :=vPos[1];
   vPos[1] :=vPos[0];
   vPos[0] :=pos[i];
   IF pos[i]=vPos[1] THEN       (*two consecutive samples equal*)
      IF pos[i]=vPos[2] THEN    (*three consecutive samples equal*)
         IF pos[i]=vPos[3] THEN (*four!--> position is really constant?!!*)
            slope:=0.0;
         END;
         pos[i]:=vPos[2]+2.0*slope; (*solution to three equal samples*)
      ELSE
         pos[i]:=vPos[1]+slope; (*solution to two equal samples*)
      END;
   ELSIF vPos[1]<>vPos[2] THEN  (*if pos(i-1)=pos(i-2)->> we can't update!*)
      slope:=pos[i]-vPos[1];    (* update of slope *)
   END;
END;
```

## A.4 Identification of Joint 1

```
%----   IDENTIFICATION OF ROBOT JOINT 1  -------

%----  m_11*qddot + d1*sign(qdot) + d2*qdot + b = u
%----  m_11=a1+a2*sin^2(q2)+a3*sin(q2)

RegOff(1);

%---- After experiments with Exc_handler

u=inp_X(1,:)';
q1=resp_X(1,:)';
q2=resp_X(2,:)';
q3=resp_X(3,:)';
q1dot=resp_X(4,:)';

%---- Filtering
tsamp=5e-3;
a=0.95;
Gfilt=tf((1-a),[1 -a],tsamp);
Gfiltd=tf([(1-a) (a-1)],[tsamp -a*tsamp 0],tsamp);
q1f=lsim(Gfilt,q1,time);
q2f=lsim(Gfilt,q2,time);
q3f=lsim(Gfilt,q3,time);
q1dotf=lsim(Gfilt,q1dot,time);
q1ddotf=lsim(Gfiltd,q1dot,time);
uf=lsim(Gfilt,u,time);

%---- Construction of the regressor
```

```
REG1=q1ddotf;
REG2=q1ddotf.*sin(q2f).*sin(q2f);
REG3=q1ddotf.*sin(q3f).*sin(q3f);
REG4=q1ddotf.*cos(q2f).*cos(q2f);
REG5=q1ddotf.*cos(q3f).*cos(q3f);
REG6=q1ddotf.*cos(q3f).*sin(q2f);
REG7=sign(q1dotf);
REG8=q1dotf;
REG9=q1ddotf.*sin(q2f);
REG10=abs(REG7);

REG=[REG1 REG2 REG9 REG7 REG8 REG10];
theta=inv(REG'*REG)*REG'*uf;

a1=theta(1);
a2=theta(2);
a3=theta(3);
d1=theta(4);
d2=theta(5);
b=theta(6);

%---- VALIDATION -------------------------------

%---- we will feed the robot model in the simulink file
%---- 'robobserver.mdl' with the real robot data
%---- and compare the output of the model with the real positions
u=J1_newexp(:,1);
q1=J1_newexp(:,2);
q2=J1_newexp(:,3);
q3=J1_newexp(:,4);
q1dot=J1_newexp(:,5);
time=(0:tsamp:(length(u)-1)*tsamp)';
%---- Defining inputs to Simulink  >> from workspace
uu=[time u];
pos2=[time q2];
pos3=[time q3];
pos1=[time q1];
vel=[time q1dot];

sim('robobserver')
```

# B. Simulink Models

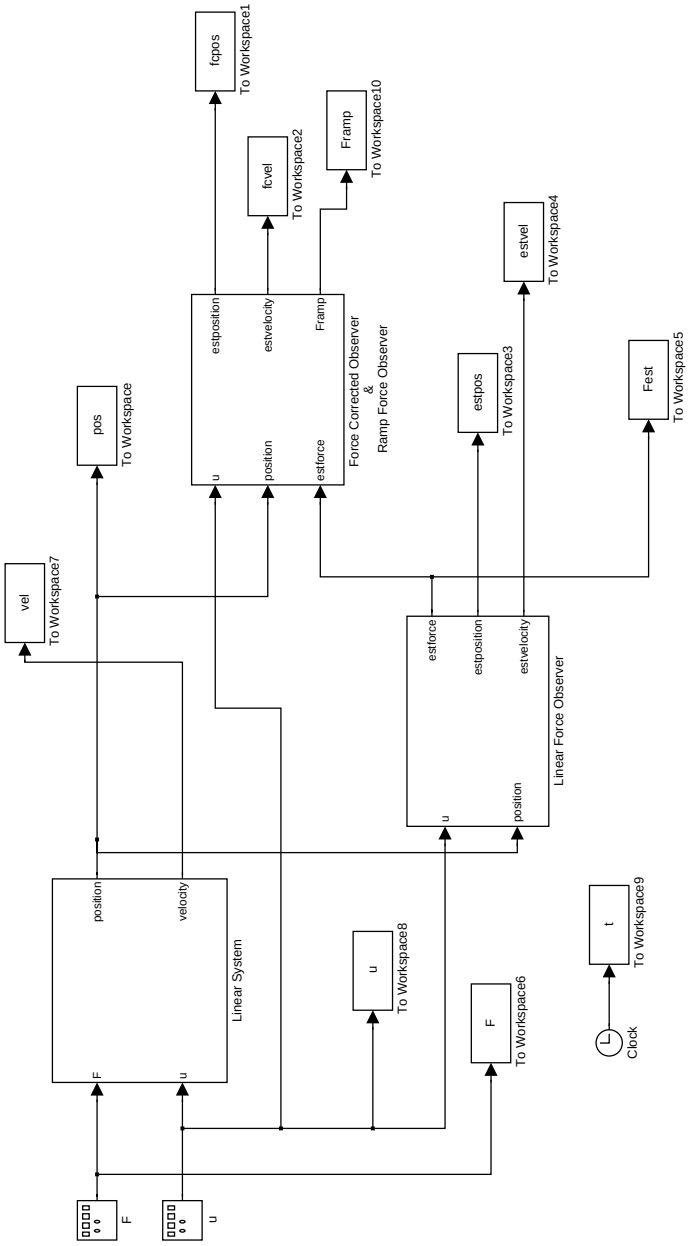


**Figure B.1** Force Observer for linear systems, Force Corrected Observer and Ramp Force Observer.

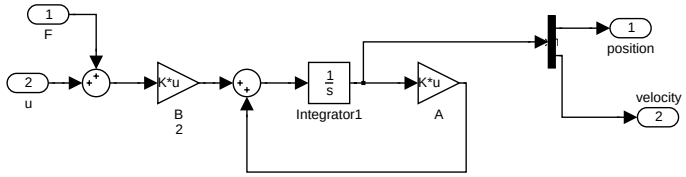


**Figure B.2** Subsystem: 'Linear System'

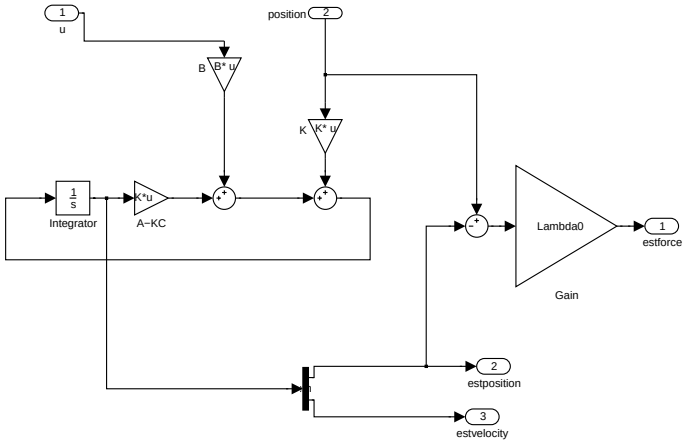


**Figure B.3** Subsystem: 'Linear Force Observer'

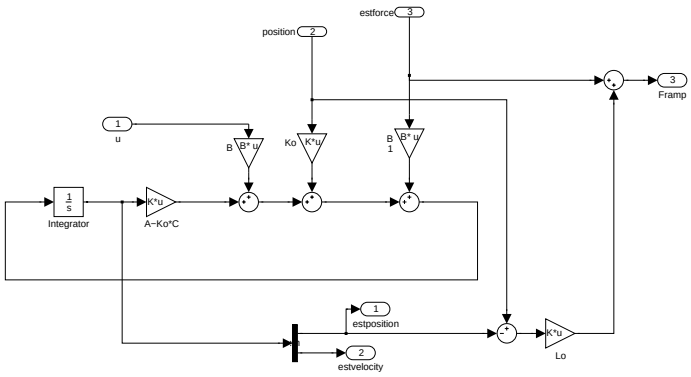


**Figure B.4** Subsystem: 'Force Corrected Observer & Ramp Force Observer'.

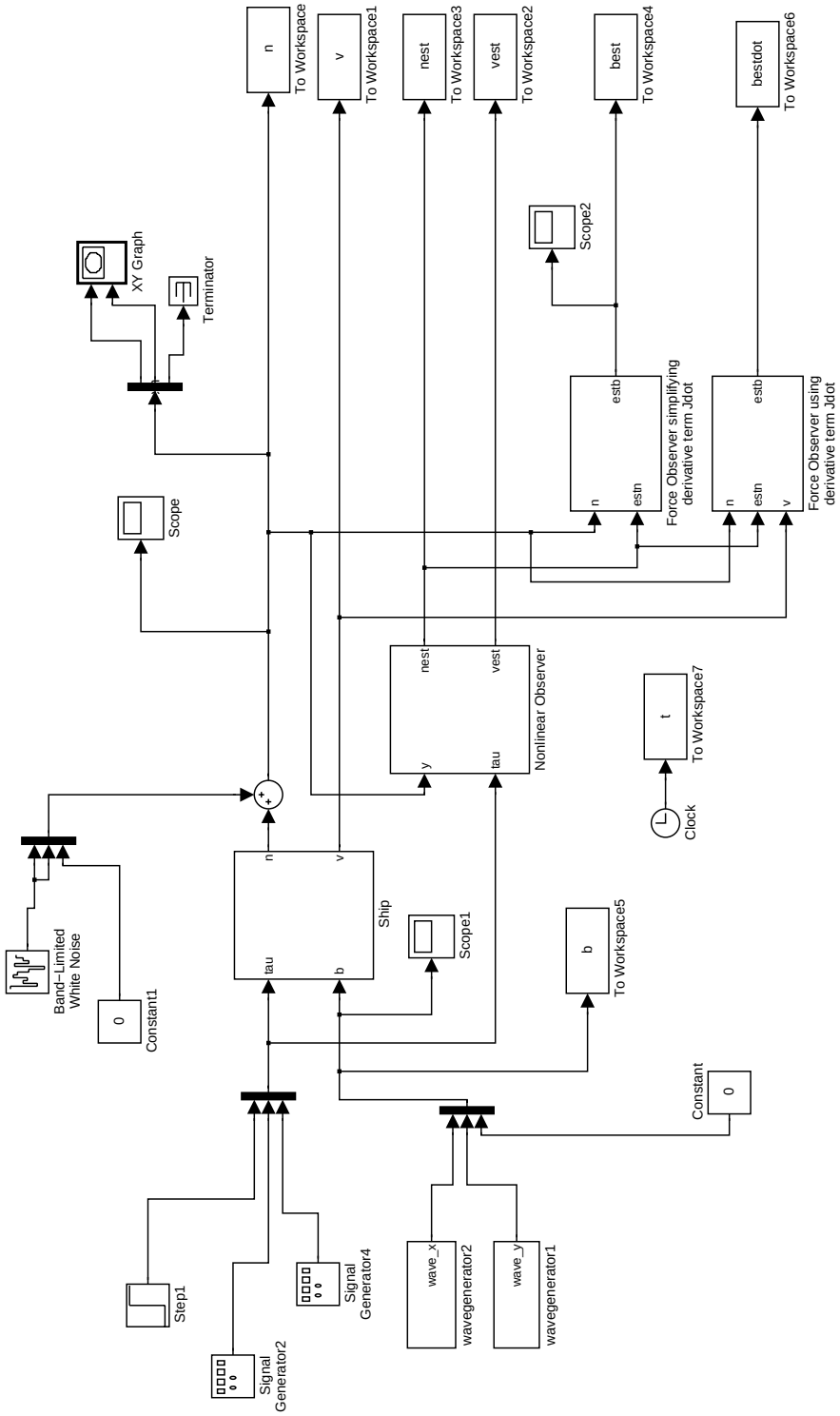


**Figure B.5** Force Observer for Ships.

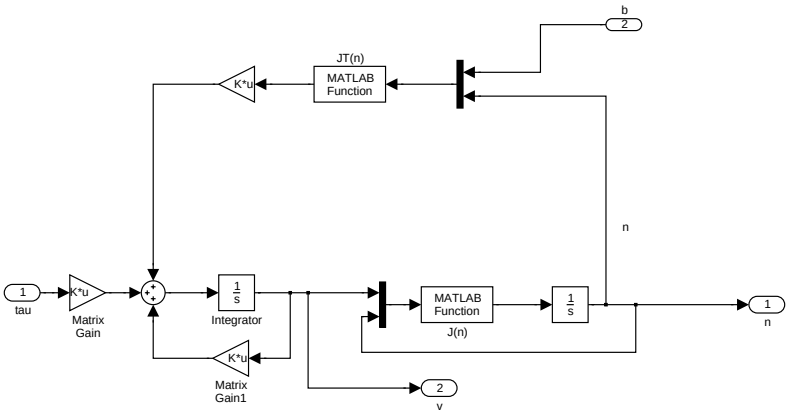


**Figure B.6** Subsystem: 'Ship'.

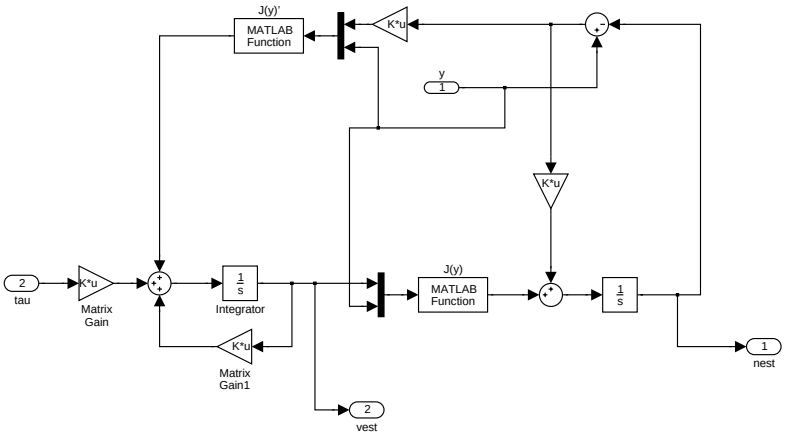


**Figure B.7** Subsystem: 'Ship nonlinear observer'.

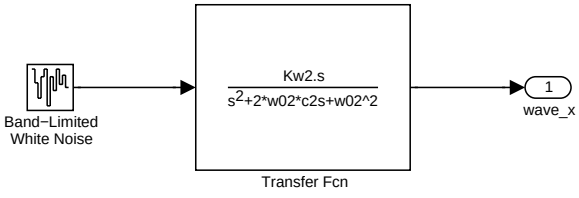


**Figure B.8** Subsystem: 'wavegenerator'.

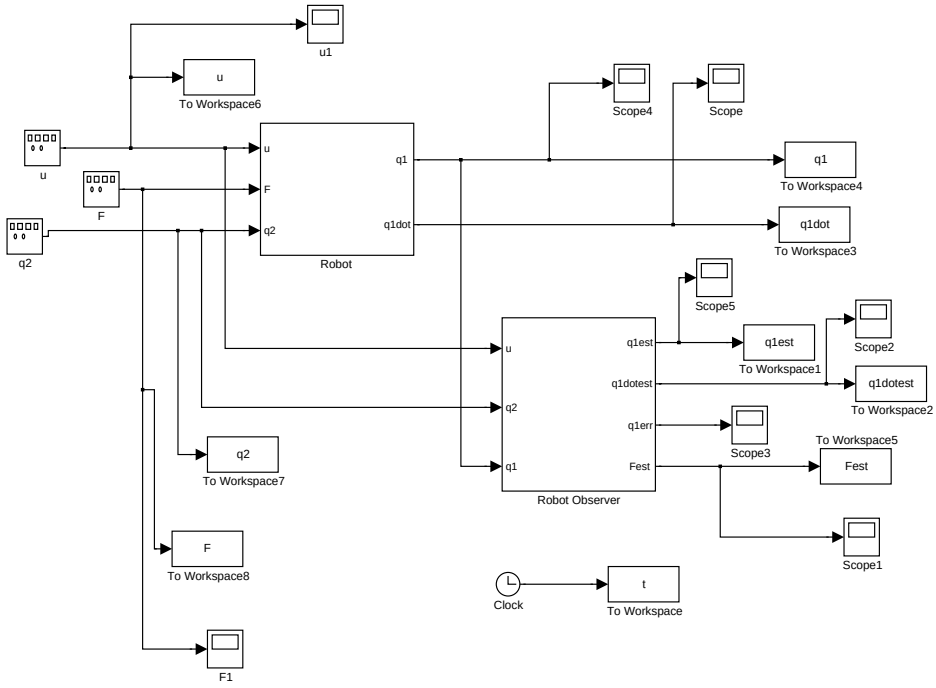


**Figure B.9** Simulink model for Robot Force Observer.

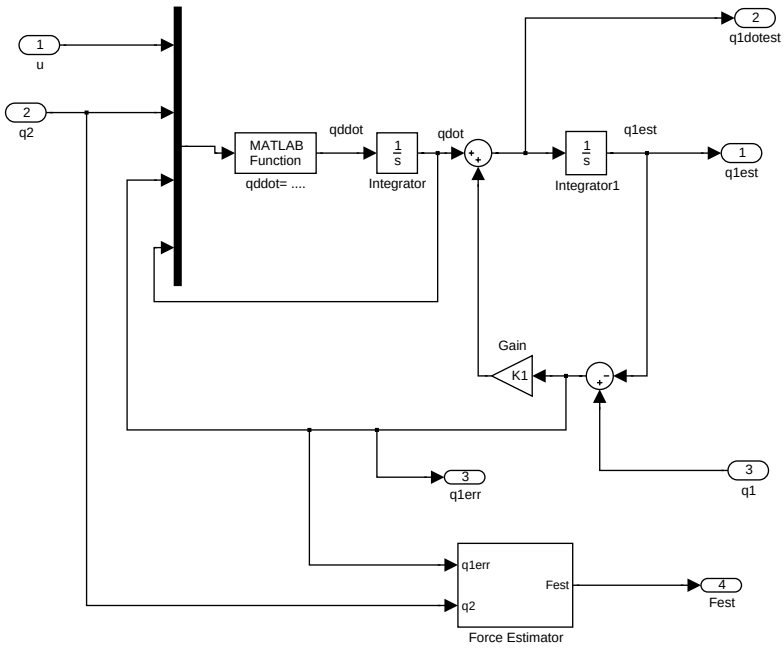


**Figure B.10** Subsystem: 'Robot Observer'.